M 2021

U.PORTO
FEUP FACULDADE DE ENGENHARIA
UNIVERSIDADE DO PORTO

Electrochemistry for Water Remediation and Energy Production

INÊS LOPES PINHO
DISSERTAÇÃO DE MESTRADO APRESENTADA
À FACULDADE DE ENGENHARIA DA UNIVERSIDADE DO PORTO EM
ENGENHARIA QUÍMICA

Master in Chemical Engineering

Electrochemistry for Water Remediation and Energy Production

Master dissertation

of

Inês Lopes Pinho

Developed within the course of dissertation

held in

Supervisor at FEUP: **Vítor Jorge Pais Vilar**

Joint supervisor at FEUP: **Maria Francisca da Costa Moreira**

Coordinator at EFACEC company: **Hugo Miguel Rodrigues Campelo**

October 2021

Acknowledgments

In this dissertation I had the opportunity to do part of my work outside of Portugal, at the University of Castilla La-Mancha (UCLM), in Spain, which I consider an excellent opportunity to enrich knowledge and acquire not only professional but also personal experience abroad. In addition, the work I did in Portugal at FEUP allowed me to expand my knowledge, laboratory practice and autonomous work capacity. All this work was done with the help and support of the people around me:

First, I would like to thank my academic supervisor at FEUP, Doctor Vítor Vilar, and my academic co-supervisor at FEUP, Doctor Francisca Moreira, for all the support provided throughout the dissertation and words of encouragement and guidance.

To Professor Justo Lobato and Manuel Rodrigo at UCLM for a very warm welcoming at a new environment, all the time disposed and for inducting me new learnings.

To coordinator at EFACEC company, Engineer Hugo Campelo, for being so receptive to help me, as well as for the opportunity of exploring this dissertation theme, that I consider very promising.

For all my colleagues from E3L lab, in UCLM, who received and welcomed me in the best way possible, especially to Andrés, for all the tutoring, help, patience, friendship and kindness, and Andrea, for all the hospitality, goodwill and amiability. As well as, colleagues from LSRE-LCM lab, in FEUP, for always being available to help, mainly to Daniela for all monitoring and assistance at all the times, and always being kind to me.

I must also thank all my close friends for always being there when I needed and for liven my days up, making this much easier.

To my dearest Luís, for always being by my side, helping me with everything and lifting me up when I needed the most, for all the patience and laughter.

And finally, to my Mom and Dad, for always being present and supportive, trusting me in all my decisions without letting me down. But also, to my brother, David, for always making me laugh and cheering me up.

Abstract

In this dissertation, electrochemical processes were applied in two distinct fields: (i) remediation of an industrial wastewater – an olive mill wastewater (OMW), and (ii) production of green hydrogen (H_2). In the treatment of the OMW, anodic oxidation (AO) process was applied at various current densities. The use of ultraviolet C (UVC) light and the addition of a salt were evaluated as well. The OMW had previously been subjected to filtration, clarification, coagulation/flocculation, and biological oxidation processes. The final goal was to achieve a wastewater in agreement with the discharge limits into the water bodies. For the H_2 production, water electrolysis based on the electrochemical step of the Westinghouse cycle was applied, using proton exchange membranes (PEM). The main goal was to assess the feasibility of using an innovative polybenzimidazole (PBI) membrane with graphene oxide (GO), further doped with phosphoric acid (H_3PO_4). The new membrane was compared to a standard PBI membrane in stability tests. Membranes were fully characterized.

AO proved to be a suitable process for the remediation of the pre-treated OMW. After 3 h of reaction, dissolved organic carbon (DOC) decays of 15%, 21%, 26% and 30% were obtained for current densities of 25, 100, 150 and 200 mA/cm^2. The use of UVC light and the addition of a salt to the wastewater did not improve the efficiency of the AO process. The hydroxyl radicals ($HO^{\bullet}$) electrogenerated at the anode (boron-doped diamond - BDD) surface proved to play a crucial role on organics oxidation. Upon 3 h of AO at 200 mA/cm^2, chemical oxygen demand (COD) and other requirements for the direct discharge of treated OMW into water bodies were not achieved. It would be necessary to extend the treatment time by AO or to apply a subsequent biological treatment to degrade the biodegradable organics generated during AO.

Water electrolysis using a PBI membrane with 2% GO provided the generation of higher amounts of H_2 and lower amounts of hydrogen sulphide (H_2S), an undesired reaction by-product, compared to the use of a standard PBI membrane, ultimately leading to a higher process efficiency. However, for the membrane thickness under study, the new membrane was mechanically unstable due to the rigidity provided by the GO, in contrast to the standard PBI membrane. The higher efficiency for H_2 production, achieved for the PBI membrane with 2% GO, can be attributed to its higher content of H_3PO_4 and higher capacity to retain this acid, which contributed to a higher conductivity. The new membrane also showed to be more chemically stable to the attack of persulphate. An additional characterization of a thermally cured PBI membrane demonstrated promising results for H_2 production.

Keywords: Olive mill wastewater; Anodic oxidation; Hydrogen production, Westinghouse cycle; Proton exchange membranes

Resumo

Nesta dissertação, foram aplicados processos eletroquímicos em duas áreas distintas: (i) remediação de uma água residual industrial – água ruça (AR), oriunda da produção de azeite, e (ii) produção de hidrogénio (H_2) verde. No tratamento da AR, o processo de oxidação anódica (OA) foi aplicado usando várias densidades de corrente. A utilização de luz ultravioleta C (UVC) e a adição de um sal foram também avaliadas. A AR tinha sido previamente sujeita aos processos de filtração, clarificação, coagulação/floculação e oxidação biológica. O objetivo final compreendeu a obtenção de uma água residual de acordo com os limites de descarga em meio hídrico. Para a produção de H_2, foi aplicada a eletrólise da água com base na etapa eletroquímica do ciclo Westinghouse, utilizando membranas de troca de protões (MTP). O principal objetivo foi avaliar a viabilidade da utilização de uma membrana inovadora de polibenzimidazol (PBI) com óxido de grafeno (OG), dopada com ácido fosfórico (H_3PO_4). A nova membrana foi comparada a uma membrana padrão de PBI em testes de estabilidade. As membranas foram caracterizadas detalhadamente.

A OA provou ser um processo adequado para a remediação da AR pré-tratada. Após 3 h de reação, foram obtidos decaimentos de carbono orgânico dissolvido (COD) de 15%, 21%, 26% e 30% para densidades de corrente de 25, 100, 150 e 200 mA/cm^2. A utilização da luz UVC e a adição de um sal à água residual não melhorou a eficiência do processo de OA. Os radicais hidroxilo ($HO^{\bullet}$) gerados eletricamente na superfície do ânodo (diamante dopado com boro) provaram desempenhar um papel crucial na oxidação dos compostos orgânicos. Após 3 h de OA a 200 mA/cm^2, não foram atingidos os requisitos de carência química de oxigénio (CQO) nem outros requisitos para a descarga direta da AR tratada em meio hídrico. Seria necessário prolongar o tempo de tratamento por OA ou aplicar um tratamento biológico subsequente para degradar os compostos orgânicos biodegradáveis produzidos durante a OA.

A eletrólise da água com recurso a uma membrana de PBI com 2% de OG proporcionou a geração de maiores quantidades de H_2 e menores quantidades de sulfureto de hidrogénio (H_2S), um subproduto indesejável da reação, em comparação com a utilização de uma membrana PBI padrão, acabando por conduzir a uma maior eficiência do processo. No entanto, para a espessura de membrana em estudo, a nova membrana provou ser mecanicamente instável devido à rigidez proporcionada pelo OG. A maior eficiência na produção de H_2 alcançada para a membrana de PBI com 2% de OG pode ser atribuída ao seu maior conteúdo de H_3PO_4 e maior capacidade para reter este ácido, o que contribuiu para uma maior condutividade. A nova membrana mostrou também ser mais estável quimicamente ao ataque do persulfato. Uma caracterização adicional de uma membrana de PBI termicamente curada demonstrou resultados promissores para a produção de H_2.

Palavras-chave: Água ruça; Oxidação anódica; Produção de hidrogénio; Ciclo de Westinghouse; Membranas de troca de protões

Declaration

I hereby declare, under word of honour, that this work is original and that all non-original contributions are indicated, and due references are given to the authors and sources

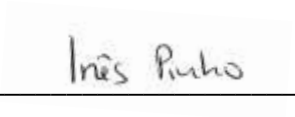

(Inês Lopes Pinho)

20th September 2021

Index

List of Figures

List of Tables

Notation and Glossary

$[DOC]_t$ DOC content after time t (mg C/L)

$[DOC]_0$ DOC content just before the reaction beginning (mg C/L)

E_{cell} Average cell voltage (V)

Flow H_2 experimental Flow of hydrogen experimental (mL/h)

Flow H_2 theoretical Flow of hydrogen theoretical (mL/h)

I Current intensity (A)

k_{DOC} Pseudo-first-order kinetic constant for DOC removal (min^{-1})

$m_{doped\ PBI}$ weight of the sample after doping and drying in the oven (g)

$m_{dry\ PBI}$ weight of the sample after drying in the oven (g)

M_{H3PO4} molecular weight of the acid used, H_3PO_4 (g/mol)

M_{PBI} molecular weight of the PBI (g/r.u.PBI)

R^2 Coefficient of determination

R_p Ohmic resistance (mΩ)

R_{ch} Charge transfer resistance (mΩ)

S^2_R Residual variance (mg^2/L^2)

t Time of reaction (h)

V_s Volume of solution (L)

List of Acronyms

ADL Acid doped level

AEMs Alkaline anion exchange membranes

AO Anodic oxidation

AOPs Advanced oxidation processes

AWE Alkaline water electrolysis

BDD Boron doped diamond

BOD_5 5-day Biological oxygen demand

COD Chemical oxygen demand

DIC Dissolved inorganic carbon

DMA N-dimethylacetamide

DOC Dissolved organic carbon

EAOPs Electrochemical advanced oxidation processes

EC Energy consumption

EF Electro-Fenton

EIS Electrochemical impedance spectroscopy

ELV Emission limit value

e- Electrons

GC/MS Gas chromatography coupled to mass spectrometry

GO Graphene oxide

$HO^{\bullet}$ Hydroxyl radicals

HyS Hybrid sulphur cycle

IR Infrared

LSV Linear scanning voltammetry

MEA Membrane electrode assemble

OMW Olive mill wastewater

PBI Polybenzimidazole

PEF Photoelectro-Fenton

PEMs Proton exchange membranes / Polymer electrolyte membrane

PTFE Polytetrafluorethylene

SOE Solid oxide electrolysis

TDC Total dissolved carbon

TSS Total suspended solids

VSS Volatile suspended solids

XDR X-ray diffractometer

1 Introduction

1.1 Water, energy and electrochemistry

Water pollution, mostly because of discharge of non-treated or unproperly treated city sewage and industrial wastewater, is severely degrading water quality. The industrial sector of food production is highly contributing to the generation of wastewater and the damaging of the water quality. One example relies on the production of olive oil, which contributes to the production of large amounts of wastewater that causes serious environmental problems if not properly treated [1]. It is urgent to provide efficient and environmentally sustainable technologies to remediate wastewater from food production, supporting both water security and agricultural practices.

On the other hand, global growth in population, economic development and urbanization are expected to double the demand for energy by 2050, according to the International Renewable Energy Agency [2]. It is then also urgent to find sustainable alternatives to fossil fuels. Green hydrogen is undoubtably the leading sustainable alternative to fossil fuels. According to the investment banking company Goldman Sachs, green hydrogen could supply up to 25% of the world's energy needs by 2050 and become a 10 trillion-dollar addressable market by 2050 [3].

Electrochemistry is a sustainable and green technology, where the use of electrons (e^-) as reagents enables chemical reactions to be performed in the absence of harmful chemicals. Electrochemical driven processes have emerged for remediation of wastewater and green hydrogen production, as well as for green organic synthesis and reduction of carbon dioxide into value products. Electrochemistry is playing a key role in environmental protection, resources recovery, and climate neutrality [4].

Concerning the wastewater treatment by electrochemical driven processes, which involves organics oxidation, electrochemical advanced oxidation processes (EAOPs) have gained increasing attention [5]. As regards the green hydrogen production, which involves water splitting into hydrogen and oxygen, electrolysis is a very promising option [6].

1.2 Application of electrochemical processes for wastewater treatment

EAOPs have received considerable attention, as they have been shown to be very efficient processes, particularly in the removal of various pollutants present in water.

The main EAOPs are peroxicoagulation, anodic oxidation (AO), electro-Fenton (EF), photoelectro-Fenton (PEF) and sono-electro-Fenton.

Through these electrochemical processes complete mineralization, reduction of toxicity, and improvement of biodegradability of wastewater can be achieved. EAOPs emerges as a promising technology for water remediation since it uses non-hazardous chemicals, have low operating cost, are simple processes and show high efficiency in pollutants removal [7].

EAOPs are a subcategory within advanced oxidation processes (AOPs), which have emerged to fill the gap between the treatability achieved by conventional physicochemical and biological treatments and to meet the more stringent limits implemented by environmental regulations [8].

Usually, physical, chemical and biological processes are combined with each other to treat several kinds of wastewater, achieving good removal efficiencies. In case of the presence of recalcitrant anthropogenic pollutants in the wastewater, the application of AOPs, including EAOPs, is a promising alternative to achieve proper treatment [9, 10].

AOPs/EAOPs depend on the generation of hydroxyl radicals ($HO^{\bullet}$) and other reactive species, which are powerful oxidants able to transform recalcitrant pollutants into more biodegradable molecules or even achieve mineralization. These processes are mainly applied in the treatment of industrial wastewater coming from textile, wine, pharmaceutical, and olive oil industries, and in the treatment of leachates, among others [9].

1.2.1 Processes applied to olive mill wastewater treatment

Olive oil production has great economic importance for the Mediterranean countries, since it is in these countries that the largest quantities of olive oil are produced. In this industry, two main types of waste are produced, a solid, called pomace, and a liquid, the olive mill wastewater (OMW) [1].

The region most affected by this problem, worldwide, is the Mediterranean region, as it accounts for 75% of the world's total olive oil production, which leads to a large production of wastewater from industrial olive mills in these countries. It is estimated that about 30 million m^3 of this effluent is generated annually in this region [1].

This liquid waste is characterized by a complex mixture of recalcitrant organic compounds, representing a serious threat to the environment if not properly treated. The wastewater presents an acidic pH, between 3 and 6, high organic load (Chemical Oxygen Demand (COD) higher than 80-200 g/L), high content of biodegradable organics (5-day Biological Oxygen Demand (BOD_5) higher than 12-60 g/L), and high content of compounds inhibiting microbial growth, such as phenolic compounds (between 19-22 mg/L) and tannins [2, 11]. This effluent also contains high levels of organic matter and turbidity, which cause poor oxygenation and light penetration [12]. This effluent usually contains about 5.9-103.2 g/L of total suspended solids (TSS) and 2.4-89.9 g/L of volatile suspended solids (VSS) [13]. A multistage treatment strategy is normally required for the treatment of OMW, combining

coagulation/flocculation/sedimentation, biological oxidation and even advanced treatment technologies, such as membrane filtration, ozonation, AOPs and EAOPs [1, 14, 11, 15]. Fenton, photo-Fenton, AO, EF and PEF are the AOPs/EAOPs must applied [10] [16]. For example, the EF process, using a carbon felt electrode, showed 80% mineralization after 6 h of reaction, consuming an electrical charge of 4000 C. For the PEF process, with the use of UVC light, 90% mineralization was achieved after 3 h of reaction, consuming an electrical charge of 2000 C [10].

1.2.1.1 Anodic Oxidation

AO is the simplest and most popular EAOP. Organics can be oxidised by three main mechanisms [17]: (1) directly on the anode surface by electron transfer according to Eq. (1), (2) indirectly by heterogeneous reactive species produced as intermediates of water oxidation, including powerful physisorbed $HO^{\bullet}$ at the anode surface, denoted $M(HO^{\bullet})$, generated via Eq. (2), H_2O_2 produced from $M(HO^{\bullet})$ dimerization according to Eq. (3), and O_3 generated from water discharge at the anode surface via Eq. (4), and (3) indirectly by oxidants electrochemically produced from species existing in the bulk solution.

$$R \rightarrow (R^{\bullet})^{+} + e^{-} \quad (1)$$

$$M + H_2O \rightarrow M(HO^{\bullet}) + H^{+} + e^{-} \quad (2)$$

$$2M(HO^{\bullet}) \rightarrow 2M + H_2O_2 \quad (3)$$

$$3H_2O \rightarrow O_3 + 6H^{+} + 6e^{-} \quad (4)$$

The efficiency of AO depends mainly on the mass transfer of pollutants from the bulk to the anode surface or its vicinity. The nature of the material by which the anode is formed also shows a strong influence on the efficiency and selectivity of AO.

The interaction of $M(HO^{\bullet})$ with the anode surface is considered to be responsible for the existence of two types of anode materials: so-called active anodes, with low O_2 potentials, and so-called non-active anodes, with high O_2 potentials.

In active anodes, the $M(HO^{\bullet})$ is transformed into a higher state oxide or superoxide MO via Eq.(5) [17], and in non-active anodes the $M(^{\bullet}OH)$ is so weakly physiosorbed on the anode surface that it can react with organics, providing their oxidation.

$$M(HO^{\bullet}) \rightarrow MO + H^{+} + e\text{-} \quad (5)$$

It is known that the higher the O_2 evolution potential of the anode material, the weaker is the interaction of $M(^{\bullet}OH)$ with the anode surface and the higher is the chemical reactivity for organic oxidation.

Some typical active anode electrodes are ruthenium dioxide (RuO_2), iridium dioxide (IrO_2), platinum (Pt), graphite and other sp^2 (carbon-based electrodes). These shows potential for O_2 evolution generally below 1.8 V/SHE.

On the other hand, lead dioxide (PbO_2), tin dioxide (SnO_2) and boron doped diamond (BDD) electrodes can be considered as non-active electrodes, showing O_2 evolution potential from 1.8 to 2.6 V/SHE. Thus, the BDD anode is considered the most suitable anode for AO, since it is the most powerful non-active anode known [5]. Table 1.1 shows the potential for O_2 evolution of various anode materials used in AO.

Table 1.1 - Potential for O_2 evolution of various anode materials used in AO [5].

Anode material	Potential for O_2 evolution (V/SHE)
RuO_2	1.4-1.7
IrO_2	1.5-1.8
Pt	1.6-1.9
Graphite	1.7
PbO_2	1.8-2.0
SnO_2	1.9-2.2
BDD	2.2-2.6

AO can be further enhanced by the action of oxidants such as persulphate ($S_2O_8^{2-}$), active chlorine species, and sulphate radicals ($SO_4^{\bullet-}$), which are electrochemically generated from existing agents in solution. The salts may already make up the wastewater matrix or alternatively may be added externally.

In the case of $S_2O_8^{2-}$, it can be efficiently produced from sulphate ions (SO_4^{2-}) by Eq.(6) [17], using only non-active anodes such as BDD and PbO_2.

$$2SO_4^{2-} \rightarrow S_2O_8^{2-} + 2e^- \quad (6)$$

Active chlorine species (chlorine – Cl_2, hypochlorous acid – HClO, and hypochlorite ion – ClO^-) can be generated from chlorine ions (Cl^-) via Eqs. (7)-(9) [13, 14] .

$$2Cl^- \rightarrow Cl_2 + 2e - \quad (7)$$

$$Cl_2 + H_2O \rightarrow HClO + Cl^- + H^+ \quad (8)$$

$$HClO \rightarrow ClO^- + H^+ \quad (9)$$

The active chlorine species that are predominantly formed along the AO depends on the pH of the effluent. Up to pH 3, the predominant active chlorine species is Cl_2, from pH 3 to 8 the dominant one is HClO and for pH above 8, ClO^- prevails. ClO^- (E^o = 0.89 V/SHE) presents lower redox potential than

HClO (E^o = 1.49 V/SHE) and Cl_2 (E^o = 1.36 V/SHE), thus the oxidation of organics should be faster in acidic than in alkaline media [5].

$SO_4^{\bullet -}$ are able to be produced by various pathways, such as SO_4^{2-} oxidation at the surface of non-active anodes via Eq. (10) [19], $S_2O_8^{2-}$ reaction with $HO^\bullet$ or an organic *R* via Eqs. (11) or (12) [20], and $S_2O_8^{2-}$ cathodic reaction via Eq. (13) [21].

$$SO_4^{2-} \rightarrow SO_4^{\bullet -} + e^- \quad (10)$$

$$S_2O_8^{2-} + HO^\bullet \rightarrow HSO_4^- + SO_4^{\bullet -} + 1/2O_2 \quad (11)$$

$$S_2O_8^{2-} + R \rightarrow 2SO_4^{\bullet -} + (R^\bullet) \quad (12)$$

$$S_2O_8^{2-} + e^- \rightarrow SO_4^{2-} + SO_4^{\bullet -} \quad (13)$$

The major drawback of AO in the presence of active chlorine is the formation of organochlorine species (chloramines, trihalomethanes, haloacetonitriles, and haloketones), which are very toxic and generally more recalcitrant than the parent molecules. The formation of these organochlorine products during AO has been detected due to the reaction of active chlorine species with different functional groups of organic matter.

To improve the efficiency of the AO, UVC light can be added since it may directly provide the photolysis of some organic matter and/or decompose some electrogenerated by-products, such as H_2O_2, O_3, $S_2O_8^{2-}$ and HClO, into powerful oxidants, such as $HO^\bullet$, $SO_4^{\bullet -}$ and chlorine radical ($Cl^\bullet$), according to Eqs. (14) [22], (15) [23], (16) [24] and (17) [25].

$$H_2O_2 + h\nu \rightarrow 2HO^\bullet \quad (14)$$

$$O_3 + H_2O + h\nu \rightarrow 2HO^\bullet + O_2 \quad (15)$$

$$S_2O_8^{2-} + h\nu \rightarrow 2SO_4^{\bullet -} \quad (16)$$

$$HClO + h\nu \rightarrow HO^\bullet + Cl^\bullet \quad (17)$$

A flow electrolytic cell with internal recirculation was successfully used for the treatment of a OMW, showing almost complete degradation of phenols using the AO process, with treatment times up to 60 min. Regarding COD removal, this was relatively low as it never exceeded 40% even after prolonged times (up to 240 min of reaction). However, as the reaction proceeded, the toxicity increased due to the formation of organochlorine by-products, as confirmed by GC/MS analysis (Gas chromatography coupled to mass spectrometry) [26].

1.3 Application of electrochemical processes for production of hydrogen

1.3.1 Hydrogen as a new energy source

In an attempt to replace primary energy from fossil fuels in the future, more and more renewable and clean energy sources have been used. Worldwide there has been a great demand for these energy

sources, and among many others, H_2 has emerged. H_2 has proven to be a very suitable energy carrier and this new form of energy is growing a lot globally [27].

Among several technologies for H_2 production, water electrolysis using electricity from renewable sources is the most basic and conventional. In this process, water molecules are transformed into hydrogen and oxygen according to equation Eq.(18) [6]:

$$H_2O\ (l) \rightarrow H_2\ (g) + ½\ O_2\ (g) \quad (18)$$

Energy is required for this reaction to occur, preferably from a renewable energy source. During the reaction, it is also necessary to add an electrolyte, since at ambient temperature, pure water is a very weak conductor of electricity. This electrolyte can be an acid or a base and serves only to improve the conductivity of water by forming ions that easily conduct electricity in solution, flowing from one electrode to the other. An example of a widely used electrolyte is NaOH.

Thus, based on the electrolyte used, water electrolysis technology can be divided into four main classifications: alkaline water electrolysis (AWE), proton exchange membranes (PEMs), alkaline anion exchange membranes (AEMs) and solid oxide water electrolysis (SOE). The principles of operation are the same for all of them [6].

1.3.2 Westinghouse cycle

To improve the efficiency of the water electrolysis process, one of the most promising and sustainable ways is to combine the electrolytic process with other non-electrochemical processes, as is the case of the Westinghouse cycle, also known as the Hybrid Sulphur cycle (HyS). This process is composed of an electrochemical stage and a thermochemical stage. In the electrochemical step, H_2O and sulfur dioxide (SO_2) are used to produce hydrogen (H_2) and sulfuric acid (H_2SO_4). Some heat (80-120 ºC) is required in this process, so that the SO_2 is depolarized. At the anode of the cell, SO_2 is electrochemically oxidised to form H_2SO_4, electrons, and protons via Eq. (19) [27]. These protons formed at the anode go to the cathode, conducted through an electrocatalytic separator, where they recombine with the electrons and form H_2 via Eq. (20) [27].

$$SO_2\ (aq) + 2H_2O\ (l) \rightarrow H_2SO_4\ (aq) + 2H^+ + 2e^- \quad (19)$$

$$2H^+ + 2e^- \rightarrow H_2\ (g) \quad (20)$$

In the thermochemical step, common in all sulphur-based thermochemical cycles, the decomposition of H_2SO_4 produced in the electrochemical step takes place. The H_2SO_4 is vaporised (at approximately 900 ºC) and superheated (at approximately 1170 ºC) and decomposes into sulphur trioxide (SO_3) and H_2O via Eq. (21) [27]. Next, another reaction occurs, the catalytic decomposition of SO_3 via Eq. (22)

[27], where SO_2 and O_2 are produced. Energy sources, such as nuclear and solar energy, are used to reach these high temperatures.

$$H_2SO_4\ (aq) \rightarrow SO_3\ (g) + H_2O\ (g) \quad (21)$$

$$SO_3\ (g) \rightarrow SO_2\ (g) + \tfrac{1}{2}\ O_2\ (g) \quad (22)$$

This SO_2 produced in the thermochemical step, can be reused again as a reactant in the electrochemical step, hence the name "cycle". In addition, O_2 is produced, which can be used for other applications [27]. Figure 1.1 shows the scheme of the Westinghouse cycle.

In this dissertation, only the electrochemical part of the system was performed, using SO_2 from a SO_2 tank, but discarded SO_2 from industries, as waste, could be used. Thus, this process is very advantageous, since H_2 is produced and there is the possibility of reducing the amount of this toxic gas, SO_2, by using it as a reagent. Furthermore, it is produced H_2SO_4, which can be sold, as it is a very common and expensive acid used in different processes.

The Westinghouse cycle can also use renewable energy as an energy source. Furthermore, what makes this process interesting and different from many others, is the low power consumption, since the depolarisation electrolysis of SO_2 is performed at a low theoretical cell potential of 0.158 V, compared to conventional water electrolysis of 1.23 V [27].

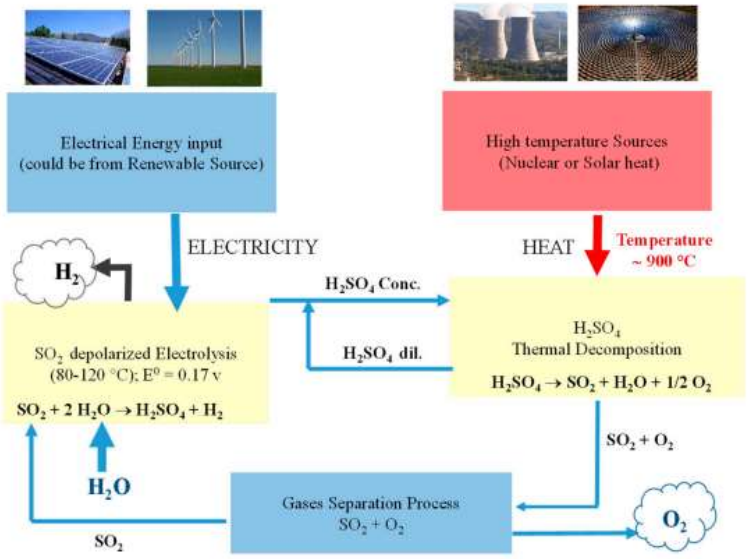

Figure 1.1 - Scheme of the Westinghouse cycle (Reprinted from Díaz-Abad et al. [27], Copyright 2019).

1.3.3 Polymer electrolyte membrane electrolysis

Alkaline electrolysis is considered the most traditional and simplest H_2O electrolysis process. This process is characterized by having an alkaline liquid electrolyte consisting of a caustic potassium solution at a level of 20 to 30% potassium hydroxide (KOH), in which two electrodes are immersed.

These electrodes are separated by a diaphragm, which is intended to keep the product gases separate from each other in order to maintain efficiency and safety. In addition, the diaphragm must be permeable to hydroxide ions (HO^-) and H_2O molecules. However, the H_2 production throughout alkaline electrolysers have some bottlenecks, such as: (i) limited current density, because the diaphragm and electrolytes suffer high ohmic losses, which leads to a low maximum achievable current density; (ii) low partial charge range, which means that the diaphragm does not completely prevent product gases from dispersing across it and, thus, oxygen diffusion occurs in the cathode chamber, reducing the efficiency of the electrolyser, and (iii) low operating pressure of the liquid electrolyte, which makes the stack configuration bulky [28].

In order to overcome these limitations, polymer electrolyte membrane (PEM) electrolysis, also known as proton exchange membrane, has been applied. The mechanism of operation of a PEM water electrolysis cell is shown in Figure 1.2.

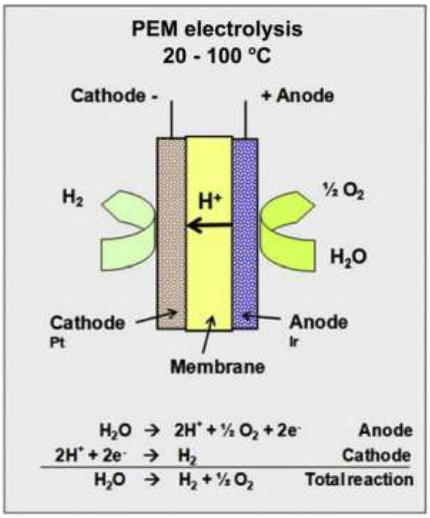

Figure 1.2 - Schematic of the operating principle of a PEM water electrolysis cell (Reprinted from Carmo et al. [28], Copyright 2013).

This electrolyser contains a solid polymer electrolyte, which started out as a solid sulfonated polystyrene membrane and more recently has been a polymer electrolyte membrane (Nafion, fumapem) that provides high proton conductivity, high pressure operation, compact system design and low gas conductivity. The fact that the membrane is very thin (20-300 μm) is one of the reasons for all advantages of the solid polymer electrolyte. Other advantages of the PEM are: the ability to achieve high current densities and voltage efficiency, a good partial load range, a rapid system response, a high gas purity and a dynamic operation [28].

Nafion membranes, the most applied ones, have some disadvantages, such as decreased performance when exposed to high acid concentrations and the inability to operate at high temperatures.

Furthermore, these membranes are very expensive. [27]. Nowadays, of all the polymers that have applied, the most promising is polybenzimidazole-based membranes (PBI). PBI is an amphoteric species, which means that it can react either as an acid or base, depending on whether it is in the presence of an acid or a base. In this case PBI will react as a base. This polymer is easily doped with a strong acid and is relatively low cost. Various acids were tested to dope these membranes such as H_2SO_4, hydrochloric acid, nitric acid, phosphoric acid (H_3PO_4), and perchloric acid. The H_3PO_4 was the one that at high temperatures showed to have more thermal, chemical, and electrochemical stability, and low volatility at temperatures above 150 ºC. Furthermore, for PBI membranes doped with this acid, a significantly low water content is required for conductivity (proton transport) [29].

In the case of the Westinghouse cycle, since PBI membranes can resist to high temperatures (100-200 ºC), they are able to produce high concentrations of H_2SO_4, working at high current densities. Thus, the efficiency of this stage of the cycle is improved since high temperatures decrease voltage losses (e.g., kinetic and ohmic resistances) and, consequently, the acid concentration produced could be higher [27].

1.4 Objectives

The present dissertation was focused on the application of electrochemical processes for two main purposes: (i) remediation of an OMW, with focus on the AO process, aiming the discharge of the treated wastewater into the environment, and (ii) generation of green H_2, using PEM electrolysis (as the electrochemical step of the Westinghouse cycle), aiming to assess the feasibility of employing innovative PBI membranes doped with graphene oxide (GO).

The OMW had previously been subjected to filtration, clarification, coagulation/flocculation, and biological oxidation processes. The remediation of the pre-treated OMW was carried out by AO in an electrochemical filter-press cell equipped with a BDD anode. Various current densities were tested, as well as the presence of UVC light and the addition of a supporting electrolyte. This part of the work was carried out at the Associate Laboratory LSRE-LCM (Laboratory of Separation and Reaction Engineering and LCM - Laboratory of Catalysis), Department of Chemical Engineering, Faculty of Engineering of University of Porto (FEUP), Portugal.

In PEM electrolysis for H_2 formation, the assessment of the stability of two membranes was under focus: PBI standard membrane and PBI membrane with 2% GO, both doped with phosphoric acid. Furthermore, these two membranes as well as a thermally cured PBI membrane, also doped with phosphoric acid, were fully characterised. This part of the work was developed at the Environmental and Electrochemical Engineering Lab (E3L), Department of Chemical Engineering, University of Castilla-La Mancha (UCLM), Spain, where a two-months internship was performed.

1.5 Presentation of the company

EFACEC is a Portuguese company with a strong export profile and is present internationally, with several subsidiaries in over 65 countries.

At the end of 2014, EFACEC became its own group of companies that brings together all the means of production, technologies, and technical and human skills for the development of activities in the areas of Energy Products, Engineering, Environment, Transportation and Electric Mobility. They are therefore focused on the development of products and systems with strong added value, acting in the development of infrastructures for important sectors of economic activity.

EFACEC is considered a prestigious brand and one of the largest industrial companies in the country, above all due to its capacity for innovation. This company is based on Sustainability policies and all business management actions and practices must be based on the three dimensions of Sustainability: Governance, Environmental and Social, in order to create a sustainable business.

EFACEC gave support to this dissertation through all the knowledge on the topics here addressed provided by Doctor Hugo Miguel Rodrigues Campelo.

1.6 Contribution of the author to the work

The author carried out all experiments and analytical determinations regarding OMW treatment by AO. As regards the PEM electrolysis for H_2 production, the author performed all experiments and analytical determinations, with exception of: (i) infrared membranes characterization, (ii) quantification of phosphoric acid for membranes characterization in terms of phosphoric acid retention, and (iii) analysis of the cell purge as regards phosphates and sulphates content. These analytical determinations were carried out by a laboratory technician. The percentage of GO used for fabrication of a membrane was based on previous studies at the E3L.

The experimental units (the laboratorial scale electrochemical system for the effluent treatment and the PEM electrolyser) had already been built before this dissertation and no significant adaptation was necessary.

1.7 Organization of the dissertation

The dissertation is structured in five main chapters:

Chapter 1 corresponds to the Introduction, where it is introduced the characteristics of OMW, the technologies applied for the treatment of this kind of wastewaters, as well as a brief explanation of

the electrochemical processes in general. Furthermore, the global H_2 demand is addressed and a brief explanation of the H_2 production processes, such as water electrolysis and Westinghouse cycle. The characteristics of PBI membranes are also presented in this chapter. Finally, it is presented the objectives of this dissertation, a brief description of the company that has collaborated in this dissertation and the contribution of the author to the work.

Chapter 2, Materials and methods, describes all the chemicals and analytical determinations used in this dissertation, as well as the procedure for both type experiments and for the characterization of the membranes. The photocatalytic systems, and the mathematical model used for the determination of the kinetic constants are also included in this section.

Chapter 3 presents the experimental results and their discussion, addressing first the application of AO for remediation of the OMW and afterwards the application of PEM for H_2 production, including stability tests and membranes characterization.

Finally, Chapters 4 and 5 display, respectively, the conclusions of the obtained results, and the objectives achieved, other work carried out and some suggestions for future work.

2 Materials and Methods

2.1 Application of electrochemical processes for wastewater treatment

2.1.1 Olive Mill Wastewater

The OMW was collected from an olive oil production plant in Northern Portugal, which adopted a two-phase centrifugation process for oil extraction. It was picked 1 m deep from the storage tank. It was filtered through a 2 mm pore sieve and settled for two weeks for a better separation of its phases: (i) oil and grease, (ii) liquid phase (OMW wastewater), and (iii) sludge and solids (from the top to the bottom). Oil and grease was top removed, and the effluent supernatant was carefully withdrawn and used in this work. Before the application of the EAOP, this OMW was subjected to two treatment stages. This pre-treatment was carried out within another study and will be only briefly mentioned here. The first treatment stage comprised a coagulation/flocculation process to enable the removal of suspended solids, colour and organic matter, including phenolic compounds. The second stage comprised a biological oxidation and lasted 20 days. In this stage, the biodegradable organic content was drastically reduced, including a large removal of phenols. The main characteristics of the bio-OMW, used in this dissertation, can be accessed in Table 2.1.

Table 2.1 - Main characteristics of bio-OMW.

Parameter	Units	Bio-OMW	ELV[a]
Colour	-	Dark brown	-
Colour (1:20)	-	d.	n.d.
Colour	Pt-Co units	1520	-
pH	scale sorënsen	8.3	6.0-9.0
Conductivity	mS/cm	7.2	-
Dissolved organic carbon (DOC)	mg C/L	319	-
Chemical oxygen demand (COD)	mg O_2/L	718	150
COD/DOC	-	2.3	-
Phenols	mg C_6H_5OH/L	5.3	0.5
Turbidity	NTU	120	-
Total suspended solids (TSS)	mg/L	105	60
Volatile suspended solids (VSS)	mg/L	43	-

[a] Emission limit value (ELV) for wastewater disposal into aquatic environment imposed by the Portuguese legislation (Decree Law 236/98, 1998).
d. – detected.
n.d. – not detected.

2.1.2 Chemicals

Sodium chloride (NaCl) 100% (w/w) supplied by Merck was used as salt to provide extra conductivity to the OMW. Sodium persulphate ($Na_2S_2O_8$) ≥99% (w/w) supplied by Merck was used to test the effect

of this oxidant. Potassium iodide (KI) 100% (w/w) supplied by Merck and sodium hydrogen carbonate ($NaHCO_3$) 99%-101% (w/w) supplied by Labkem were used in the determination of the in-situ chemical oxidants. All the chemicals were used as delivered. Demineralized water was obtained by a Panice® reverse osmosis system. This water was used not only to prepare solutions but also to clean the system and all the laboratorial material.

2.1.3 Electrochemical system

Figures 2.1 and 2.2 display the sketch and the photography of the laboratorial flow system for AO trials. This system was mainly composed by (i) a traditional electrochemical filter-press cell, model MicroFlowCell supplied by ElectroCell (Denmark), (ii) a FluHelik photoreactor, (ii) a recirculation cylindrical glass vessel thermostatically controlled and magnetically stirred, and (iii) a gear pump (Ismatec, model BVP-Z), previously calibrated to work at a flow rate of 50 L/h. The MicroFlowCell was equipped with (i) a BDD anode (active area of 10 cm^2) composed of a conductive niobium sheet with 2 mm thickness coated with a BDD film of ~2 μm thickness, and (ii) a platinum (Pt) cathode (active area of 10 cm^2) composed of a conductive titanium (Ti) plate of 2.0 mm thickness two-side coated with a thin pure platinum (Pt) film of ~2.5 μm thickness. Both electrodes were supplied by ElectroCell (Denmark). The electrochemical cell was coupled to a power supply (UNI-T, model UTP3305, 0-5 A, 0-30 V) to provide constant current density, which directly displayed the applied potential of the cell. The FluHelik photoreactor mainly consisted of: (i) a cylindrical shell of borosilicate glass with inlet and outlet pipes located tangentially to the shell and perpendicularly to the fluid flow direction, at the top in opposite sides and in horizontal plane, and (ii) a concentric inner quartz tube filled with an UVC lamp of 11 W power - Philips TUV G11T5 (radiant power of ~2.5 W determined by H_2O_2 actinometry [30]). This photoreactor is described in detail elsewhere [30]. All the system units were connected by polytetrafluoroethylene (PTFE) tubing.

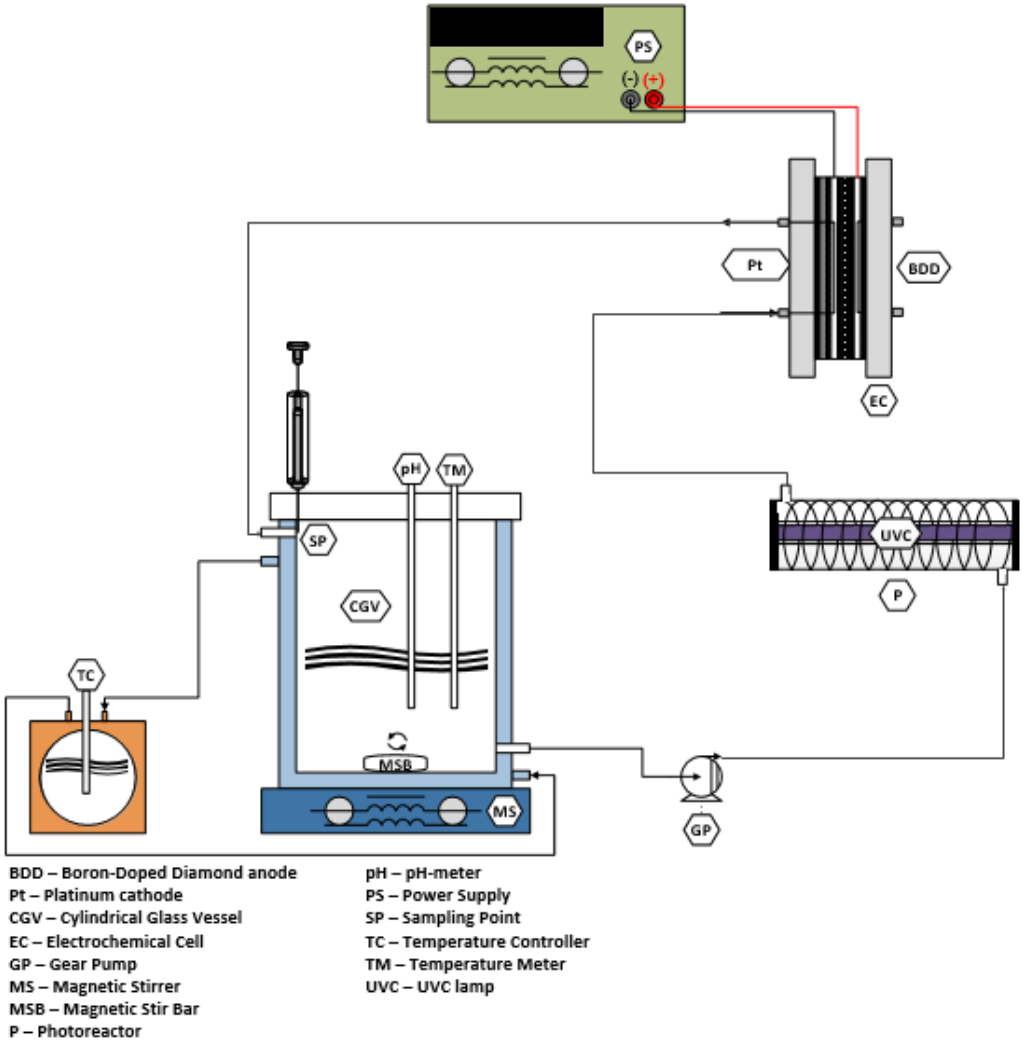

Figure 2.1 - Sketch of the laboratorial flow system for AO trials.

Figure 2.2 - Photography of the laboratorial flow system used in AO trials.

2.1.3.1 Experimental procedure

Initially, a sample of 1.1 L of the bio-OMW was taken from the storage tank with the help of a beaker and left standing until the suspended particles were deposited at the bottom. The system was already set up and all the necessary material was washed and identified.

Next, the thermostatic bath was switched on at 25ºC and the sample of effluent was placed in the homogenization vessel, as well as the probe to measure the temperature and pH of the effluent during the reaction. After that, the magnetic stirrer was turned on to try to keep the solution as homogeneous as possible, and the pump was turned on at a flow rate of 50 L/h, leaving the effluent to recirculate for about 5 min until it reached the desired temperature of 25ºC.

Immediately before starting the reaction, a first sample of 10 mL was withdrawn from the homogenization vessel, with the help of a syringe. The reaction was started by simultaneously turning on the power supply and the chronometer for 3 h. Throughout the reaction, samples were taken at the following times: 15, 30, 60, 90, 120, 150, and 180 min of reaction. For each sample taken, the temperature, pH and voltage were recorded. Additionally, dissolved organic carbon (DOC), $S_2O_8^{2-}$ and active chloride species were analysed. For DOC analysis, it was necessary to make a 5x dilution using a 25 mL volumetric flask and a well calibrated automatic pipette. For $S_2O_8^{2-}$ and active chlorine species analysis, the dilution was varied according to the different formation of these compounds. Samples were filtrated through a 0.45 µm nylon membrane filter before the analysis of DOC, $S_2O_8^{2-}$ and active chloride species concentration.

Throughout the reaction, it was necessary to control the temperature, regulating the thermostatic bath so that it was always at 25±2 ºC.

At the end of the reaction, after taking the last sample (t=180 min), the power supply and the liquid pump were turned off. The solution was emptied from the system very carefully and the system was washed, so that the next day it was ready to be used again to repeat the reaction for different conditions.

For this, the washing solution consisting of demineralized water and HCl (90% water:10% HCl by volume) was always prepared in advance, and this solution was placed in the system to recirculate for about 5 min. This solution was then removed and tap water was added, again for about 5 min, and finally demineralized water, for the same amount of time.

In the trials where UVC light was used and NaCl was added to the effluent, the procedure was the same. Except that, when starting the reaction with the UVC light, the lamp, which was inside the FluHelik, had to be turned on at the same time as the power supply and the chronometer. Since the radiation emitted by the UVC light is dangerous, it was also necessary to line the FluHelik reactor with aluminium foil so that the light would not be visible. In the test where NaCl was added to the

effluent, 3.0 g/L of NaCl had to be added to the homogenization vessel with the effluent, and before starting the recirculation of the effluent throughout the system, it was left to stir for about 10 min, to make sure that the NaCl was dissolved.

For the AO treatment, it was assessed the effect of current density (25, 100, 150 and 200 mA/cm^2), as well as the coupling to UVC light and the addition of NaCl to the bulk solution. The energy consumption for the operation of the electrochemical cell was calculated in terms of specific energy consumption per unit volume (EC, kWh/m^3) according to Eq. (23):

$$EC = \frac{E_{cell}\, I\, t}{V_s} \quad (23)$$

where E_{cell} is the average cell voltage (V), I is the current intensity (A), t is the time of reaction (h) and V_s is the volume of solution (L).

2.1.4 Analytical determinations

Table 2.2 collects the description of the various analytical determinations used throughout the experimental work of this dissertation.

Table 2.2 - Analytical determinations.

Parameter	Methodology
COD	Chemical oxygen demand (COD) was determined photometrically according to the Standard Methods for the Examination of Water and Wastewater [31], 5220 D test, by oxidation with potassium dichromate, using Merck Spectroquant® kits Cat. No. 114541, a WTW CR4200 thermoreactor and a Merck Spectroquant® Pharo 100 spectrophotometer.
Conductivity	Conductivity was determined with a HANNA Instruments HI 9828 Multiparameter analyser.
Free chlorine	Free chlorine, i.e., active chlorine species (Cl_2, HClO and ClO^-), was determined photometrically according to Standard Methods for the Examination of Water and Wastewater [31], 4500-Cl G test, by reaction with dipropyl-p-phenylenediamine, using Merck Spectroquant® kits Cat. No. 100598 and a Merck Spectroquant® Pharo 100 spectrophotometer.
Persulphate	Persulphate ($S_2O_8^{2-}$) concentration was determined photometrically according to an modified iodometric titration developed by Liang et al. [32], in which $S_2O_8^{2-}$ is determined using as reagent a solution made of water/KI (potassium iodide)/$NaHCO_3$ (sodium hydrogen carbonate) and a VWR UV-6300PC spectrophotometer set a wavelength of 352 nm.
pH	pH was measured by HI2020-02 edge from HANNA.
Phenols	Phenol and its ortho- and meta-substituted compounds were determined according to Standard Methods for the Examination of Water and Wastewater [31], 5530 C+D test, based on the reaction with 4-aminoantipyrine to form a red compound that is determined photometrically (Spectroquant® kits Cat. No. 100856 and Merck Spectroquant® Prove 300 UV/Vis spectrophotometer).
Temperature	Temperature was measured by HI2020-02 edge from HANNA.

Parameter	Methodology
Turbidity	Turbidity was measured according to the Standard Methods for the Examination of Water and Wastewater [31], 2130 B test, using a Merck Turbiquant® 3000 IR turbidimeter.
TDC **DIC** **DOC**	Total dissolved carbon (TDC) and dissolved inorganic carbon (DIC) were separately determined by catalytic combustion at 680 ºC and acidification, respectively, using a nondispersive infrared detector (NDIR) in a Shimadzu TOC-V_{CSN} analyser. Dissolved organic carbon (DOC) was given by the difference between TDC and DIC (DOC = TDC - DIC).
TSS	Total suspended solids (TSS) content was determined according to Standard Methods for the Examination of Water and Wastewater [31], 2540 D test, by filtration through a weighed standard glass-fibre filter and drying of the solid residue at 105 °C up to constant weight.
VSS	Volatile suspended solids (VSS) content was determined according to Standard Methods for the Examination of Water and Wastewater [31], 2540 E test, by ignition of the residue from TSS determination at 550 °C up to constant weight.

2.1.5 Determination of pseudo-first-order kinetic constants

A pseudo-first-order kinetic model was fitted to DOC removal data obtained along the various AO reactions, as a simple mathematical model to quantitatively compare the processes efficiency. The kinetic model was adjusted from Fig.P software for Windows from Biosoft by a nonlinear regression method. The fitting was performed by minimizing the sum of the squared deviations between experimental and predicted values. The goodness of fitting was assessed by calculating the relative standard deviations, the coefficient of determination (R^2) and the residual variance (S^2_R). The pseudo-first-order kinetic constants for DOC removal (k_{DOC}), in min^{-1}, were calculated from Equation 24:

$$[DOC]_t = [DOC]_0 \times e^{-k_{DOC} \times t} \quad (24)$$

where $[DOC]_t$ is the DOC content after time t and $[DOC]_0$ is the DOC content just before the reaction beginning.

2.2 Application of electrochemical processes for production of hydrogen

2.2.1 Chemicals

Sulphur dioxide (SO_2) 99.98% (w/w) supplied by Nippon gases was used as a reagent in the stability tests. PBI ($(C_{20}H_{12}N_4)_n$) 26% (w/w) in DMA + LiCl, DMA (C_4H_9NO) ≥ 99.5% (w/w) supplied by PanReac and pure graphene oxide ($C_{140}H_{42}O_{20}$) with a sifted of 38 μm were used in the preparation of the PBI membranes. Phosphoric acid (H_3PO_4) 85% (w/w) supplied by PanReac was used as acid to dope the PBI membranes. Pt/Vulcan (40% (w/w) in Pt) supplied by Fuel Cell Store and a PBI and DMA solution (1.5% (w/w) PBI in DMA) was used to coat the electrodes. Pure argon (Ar) was applied in the thermal cure of the membranes. Sodium persulphate ($Na_2S_2O_8$) ≥ 98% (w/w) supplied by Sigma Aldrich and sulfuric acid 1M (H_2SO_4) 95-97% (w/w) were used to characterize the membranes for chemical stability with $S_2O_8^{2-}$.

Ultrapure water was obtained by a Millipore® Direct-Q system (18.2 MΩ cm resistivity at 25 ºC). This water was used to prepare solutions, for tests carried out for the characterization of the membranes, as a reagent for the reaction, and also to clean all the laboratorial material.

2.2.2 Membranes

Three types of membranes were applied: PBI (standard), PBI with 2% GO, and thermally cured PBI, all of them doped with H_3PO_4. The former two were applied in stability tests for H_2 production, and all the membranes were fully characterized.

- Membranes fabrication

The membranes were produced using a petri dish of 14 cm diameter as mould. Then 2.6 g of PBI (and 13.5 mg of the GO, in the case of the 2% GO membrane) and 34 g of the N-dimethylacetamide (DMA), which acted as solvent, were heated until a homogeneous liquid was obtained. The mould was filled with the homogeneous liquid and placed in an oven at 80 ºC for at least 12 h. Then, the membranes were detached from the mould with the help of ultrapure water and placed in boiling water for 2 h. Finally, the membranes were dried in the oven at 80 ºC again for at least 12 h. The membranes were then ready to be cured or doped.

- Membranes thermal curing

A standard PBI membrane was thermally cured according to the procedure reported by Aili et al. [33]. A muffle was used, with a constant flow of argon and an inert atmosphere inside. The membrane was placed there for 16 h at 350 ºC. Then, the muffle was turned off and the membrane was left inside

for approximately 3 h, until the temperature fell to 100 ºC. Finally, the thermally cured membrane ready for doping was removed from the muffle.

- Membranes doping

PBI (the main component of the membranes under study) is a polymer and has no conductivity. Therefore, the PBI membranes were doped with phosphoric acid, resulting in a membrane with adequate conductivity for the electrolysis process. The PBI membrane was immersed in pure H_3PO_4, inside a beaker, and place it in the oven at 80 ºC for 12 h.

2.2.3 Electrochemical system

Figure 2.3 and 2.4 display the sketch and photography of the laboratorial single cell electrolyser. The standard PBI and PBI membrane with 2% GO, both doped with H_3PO_4, were used. For the anode and cathode, H23C2 GDL (Freudenberg, Germany), a flexible and easy to use carbon paper gas diffusion layer with a microporous layer, was used as gas diffusion and support layer. The cathode and anode, both with an active area of 25 cm^2, were prepared by sputtering a previously prepared paint with Pt/Vulcan as catalyst until a platinum loading of 0.7 mg/cm^2 Pt was achieved for both electrodes. DMA, as solvent, and a solution of PBI and DMA were used as binder with a PBI/Vulcan ratio of 1:20. A few hours before using the electrodes in the reaction, it was necessary to dope them as well. The electrodes were placed for 2 h in a muffle furnace at 180 °C and then were submersed in H_3PO_4 (10% (w/w)). To place the right amount of H_3PO_4, a scale was used and with a dropper, just 1 g of H_3PO_4 was placed evenly over the electrode. Then, the electrodes were leaving to stand for the next day.

The main electrolyser unit was coupled to a tank containing liquid H_2O, connected to a peristatic pump (Ismatec), and to a bottle of SO_2 gas, connected to a flow controller (0154 Control and read out unit by Brooks Instruments). These two components were fed to the anode of the cell. The mixture of these reactants was preheated to 109 °C to evaporate the liquid water before entering the anode of the cell. A power supply (potensiostat/galvanostat) (Autolab, model Booster20A) working in galvanostatic mode was used, directly displaying the potential of the cell. The outlet gases (H_2 and hydrogen sulphide - H_2S) were measured by gas chromatography (Shimadzu, model Nexis GC-2030), using nitrogen (N_2) as carrier gas. The H_2S was a by-product competing with the H_2 production. The ohmic resistance and charge transfer resistance values as well as the polarization curves from the characterisation were obtained through the NOVA 2.1.2 program.

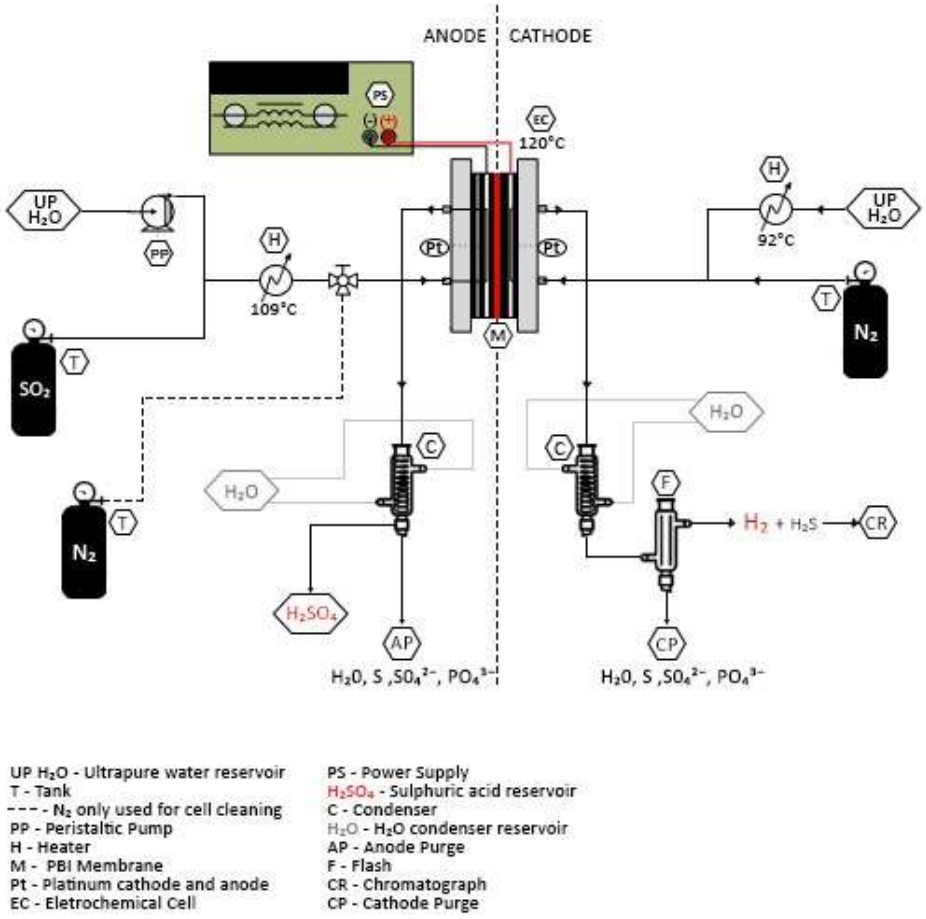

Figure 2.3 - Sketch of the laboratorial single cell electrolyser.

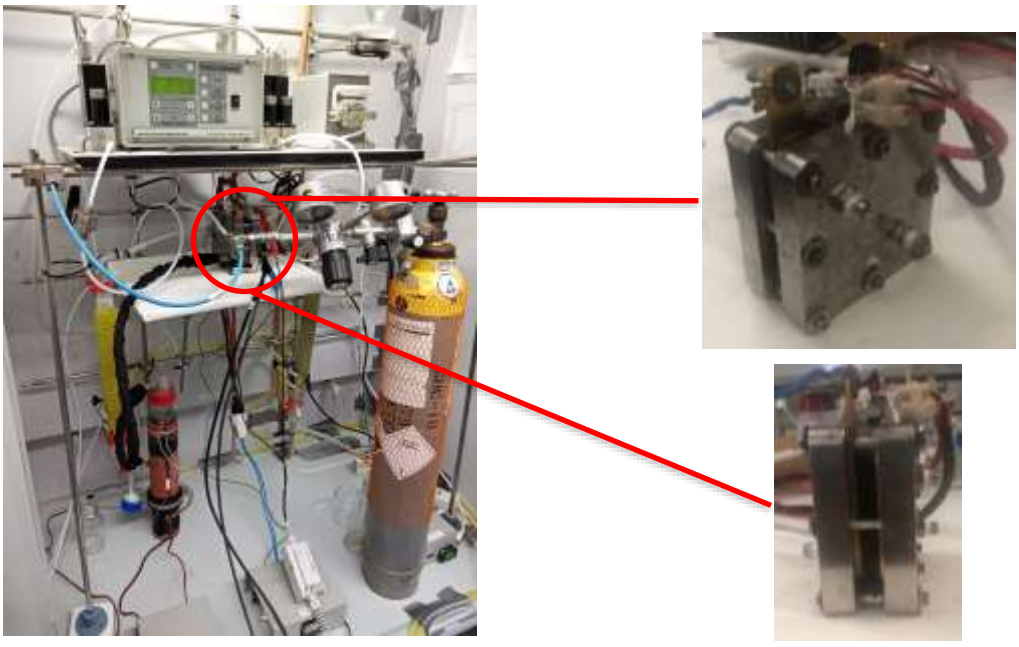

Figure 2.4 - Photography of the laboratorial single cell electrolyser.

2.2.4 Experimental procedure for stability tests of membranes with production of hydrogen

In the preliminary stability study of the membranes, for each membrane two reactions were performed, one at 110ºC and another at 120ºC, applying a constant voltage of 0.6 V. These reactions were done just to check if everything was working properly with the cell and the system, if the results obtained were the normal ones and to show how the membrane worked before starting the main experiment.

To start, the heater was turned on to heat the water in the cathode to a temperature of 92 ºC, so that it could start boiling. It is necessary to have the cathode and anode water outlet pipe insulated to ensure that the water enters the cell at the desired temperature. The cell's temperature controller was then connected, and the temperature set at 110 ºC, which is the temperature at which the first trial was performed. The cell and the source, with a constant voltage of 0.6 V, were connected immediately after connecting the source cables to the cell. Initially, only N_2 was passed throughout to clean the entire system, and for that a flow of 70 mL/min on the anode side and 100 mL/min on the cathode side was used and the N_2 valve was opened.

Finally, on the anode side, the heater was turned on to heat the anode water (reaction water) to 109 ºC to evaporate the liquid water before entering the anode of the cell and the peristaltic pump was turned on at a flow rate of 0.2 mL/min. As soon as the desired temperature was reached in the cell (110 ºC), the SO_2 bottle was opened and the N_2 valve was closed, allowing SO_2 to enter the cell. The N_2 flow rate on the anode side was changed to 0 mL/min, the SO_2 flow rate to 70 mL/min, and the N_2 flow rate on the cathode side was maintained at 100 mL/min. In the program that was connected to the system, it was possible to see a graph of I(A) *vs* t(s), shown in the results. It was expected that the steady state will be reached at around 2A after 2 h. This was the constant intensity that was applied to the system in the main experiment.

At the end of the 2 h, when the steady state was reached, a characterisation was made: polarization curves, resistances, and amount of H_2 and H_2S being produced. This electrochemical characterisation consisting of linear scanning voltammetry (LSV) and electrochemical impedance spectroscopy (EIS) was performed at the beginning and end of a day as well as throughout the day. LSVs were performed from 0.0 to 1.0 V at a scan rate of 10 mV/s. The EIS were performed at two different potentials (0.5 V and 0.7 V), and in this dissertation only the resistances obtained for 0.7 V are presented.

When a characterisation was made, samples were also taken from the outlet of the cathode and anode (anode and cathode purge), which were subsequently analysed. The trial was concluded for the temperature of 110 ºC, and then passed to the temperature of 120 ºC. For that, it was only necessary to change the temperature to 120 ºC in the cell temperature controller and wait until this temperature was reached. Then, the procedure described for 110 ºC was repeat.

After this, the main experiment was started, which was performed at 120 ºC and a current density of 80 mA/cm^2 (2A) until the membrane ruptures. It was considered that the membrane has ruptured when there was an extensive change in potential (reach 1V), which indicates that the membrane is structurally damaged and the SO_2 ions are crossing the membrane freely. The stability study had a total duration of 19 h, and the system was turned off at the end of the day and turned on again in the morning at 120 ºC at 80 mA/cm^2. Characterizations were made in the morning and at the end of the day and two more times throughout the day (before and after lunch), for each day of reaction.

Once the stability test has finished, N_2 was passed back into the system to clean it for about 15 min at a flow rate of approximately 70 mL/min.

2.2.5 Membranes characterisation procedures

The standard PBI membrane, the PBI membrane with 2% GO, and the cured PBI membrane, doped with H_3PO_4, were characterized.

- Infrared (IR)

To obtain the IR spectrum of the membranes under study, samples of non-doped membranes with the dimensions of 1x1 cm, of each of the types, were used. The analyses were carried out by a laboratory technician. These determinations were done only to confirm if the membrane had been properly cured.

- Acid doped level (ADL)

To study the amount of H_3PO_4 absorbed by the membrane, the membranes were weighed and then submerged in a H_3PO_4 solution at 80 °C in the oven for 12 h. The membranes were then dried and weighed to calculate the acid absorption using Eq. (25):

$$ADL = \frac{\frac{m_{\text{doped PBI}} - m_{\text{dry PBI}}}{M_{H_3PO_4}}}{\frac{m_{\text{dry PBI}}}{M_{\text{PBI}}}} \quad (25)$$

where $m_{\text{doped PBI}}$ is the weight of the sample after doping and drying in the oven (g), $m_{\text{dry PBI}}$ is the weight of the sample after drying in the oven (g), M_{H3PO4} is the molecular weight of the acid used, H_3PO_4 (98 g/mol), and M_{PBI} is the molecular weight of the PBI, which is a polymer and so it is actually the molecular weight of the repeating unit (308 g/r.u. PBI).

If an ADL of 10 was not reached, the previous procedure was repeated.

- Retention of phosphoric acid

To study the membranes that can retain more H_3PO_4, samples of the membranes, with the dimensions of 1x1 cm, were first washed with ultrapure water, dried, and weighed. Then, 100 mL of ultrapure

water was placed in a bottle with a magnetic stirrer and heated to 80 ºC. Then, the membranes were placed into the bottle and 1 mL of water was removed from the inside of the bottle every 10 min (also removed for *t*=0 min). The test ended when the sample for *t*=60 min was removed. It was important to keep the temperature during the whole test at 80°C, so a thermometer was used. These samples were then analysed by a laboratory technician, in terms of H_3PO_4 content.

- Chemical stability to the attack of persulphate

To verify the resistance of membranes to $S_2O_8^{2-}$ attack, a by-product that can damage the membranes, samples with dimensions of 1x1 cm from a non-doped membrane were used. It started by washing with ultrapure water, weighing, and measuring the thickness of the membranes and taking pictures always before and after the test, to see the changes in the membranes. Then, a solution with 100 mL of 1M H_2SO_4 and 50 mg of $Na_2S_2O_8$ was prepared and the membranes were placed into it. The test was performed at 80 ºC in the oven for 24 h. If at the end of the 24 h the membrane remained intact (without breaking), the test was repeated until it finally broke.

3 Results and discussion

3.1 Application of electrochemical processes for wastewater treatment

Figure 3.1 shows the effect of current density (from 25 to 200 mA/cm^2) on the AO process, as well as the effect of adding UVC light and NaCl to the AO process, in terms of DOC decay and formation of $S_2O_8^{2-}$ and active chlorine species (Cl_2, HClO and ClO^-). The corresponding k_{DOC} can be accessed in Table 3.1.

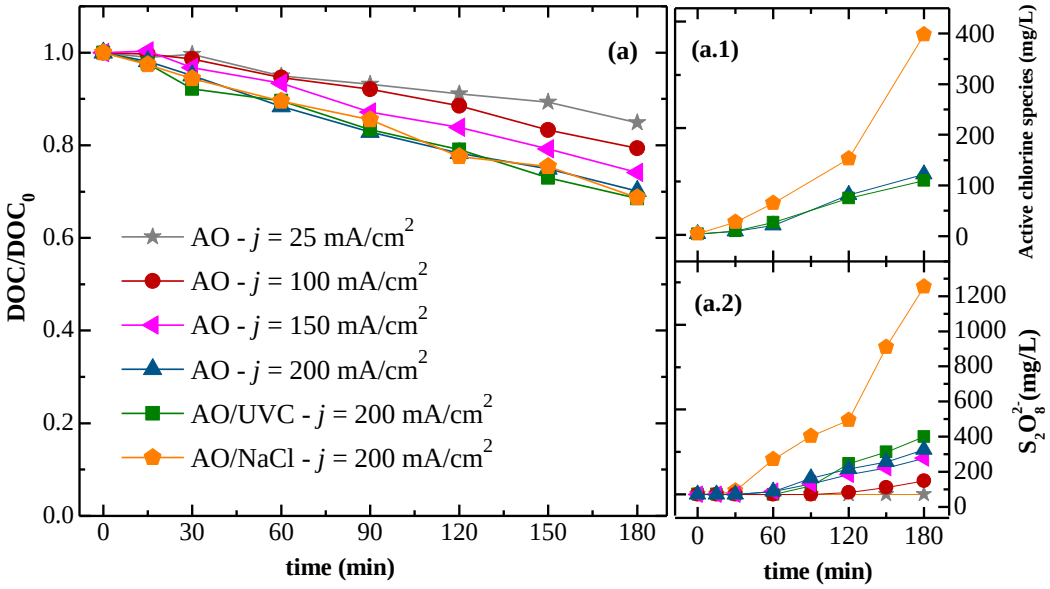

Figure 3.1 - Evolution of normalized DOC removal (a), concentration of active chlorine species (a.1) and concentration of $S_2O_8^{2-}$ (a.2) as a function of time for the treatment of the bio-OMW by AO. (★) AO at 25 mA/cm^2, (●) AO at 100 mA/cm^2, (◀) AO at 150 mA/cm^2, (▲) AO at 200 mA/cm^2, (■) AO/UVC at 200 mA/cm^2, (⬟) AO/NaCl at 200 mA/cm^2. Operational conditions: pH = natural (7.5-8.4), T = 25 ºC, 11 W UVC lamp, 3.0 g/L NaCl.

Table 3.1 - Pseudo-first-order kinetic constants for DOC removal (k_{DOC}) along with the corresponding S^2_R and R^2 obtained for the treatment of the bio-OMW by AO under conditions of Figure 3.1.

Reaction	k_{DOC} (min^{-1})	S^2_R (mg^2/L^2)	R^2	Time interval of the adjustment (min)
AO - 25 mA/cm^2	0.83 ± 0.03	11	0.982	0-15,60-180
AO - 100 mA/cm^2	1.14 ± 0.06	63	0.959	0-180
AO - 150 mA/cm^2	1.54 ± 0.06	35	0.982	0,30-180
AO - 200 mA/cm^2	1.98 ± 0.03	12	0.996	0-180
AO/UVC - 200 mA/cm^2	2.06 ± 0.05	24	0.993	0-180
AO/NaCl - 200 mA/cm^2	1.98 ± 0.05	32	0.990	0-180

By analysing Figure 3.1(a), it can be inferred that the increase of the current density provided sharper DOC removals. This was corroborated by the k_{DOC} values. The k_{DOC} was 2.4-fold higher for AO at 200

mA/cm^2 compared to AO at 25 mA/cm^2. After 3 h of reaction, DOC removals of 15%, 21%, 26% and 30% were obtained for 25, 100, 150 and 200 mA/cm^2. These results can be attributed to the occurrence in higher extent of the direct e^- transfer from the organics to the anode via Eq. (1) and/or the production of higher amounts of oxidative species, such as M($HO^\bullet$), H_2O_2, O_3, active chlorine species, $S_2O_8^{2-}$ and/or $SO_4^{\bullet-}$ via Eqs. (2)-(4) and (6)-(13) that may be able to attack the bio-OMW organics and/or the organic by-products generated during the AO process. Figure 3.1(a.1) confirms the production of active chlorine species for AO at 200 mA/cm^2. After 180 min of reaction, there was around 100 mg/L of active chlorine species. Figure 3.2 shows the relative distribution of main aqueous chlorine species as a function of pH at 25 ºC. In this case, it does not contain the same ions in solution as those under study, but the behaviour is expected to be quite similar. Therefore, it can be concluded that ~50% of HClO and ~50% of ClO^- may have been formed during the AO processes, since the pH of the OMW was ~8. As previously mentioned, HClO is the most powerful free chlorine species [18]. Furthermore, Figure 3.1(a.2) indicates the generation of increasing amounts of $S_2O_8^{2-}$ for raising current densities. However, these latter results should be analysed with precaution. $S_2O_8^{2-}$ content was determined by iodometric titration, which is a well-known method for the determination of active chlorine species, H_2O_2, O_3, among other in-situ chemical oxidants that may have inferred in the readings, giving rise to $S_2O_8^{2-}$ contents larger than the real ones. Beyond that, an additional blank experiment with the addition of 1000 mg/L of $S_2O_8^{2-}$ in the presence of UVC light provided null DOC removal (data not shown), indicating the inability of this oxidant and of UVC light to the degradation of the organics in the bio-OMW. Thus, even in the case of generation of high amounts of $S_2O_8^{2-}$, the role of this oxidant in organics oxidation must have been poor.

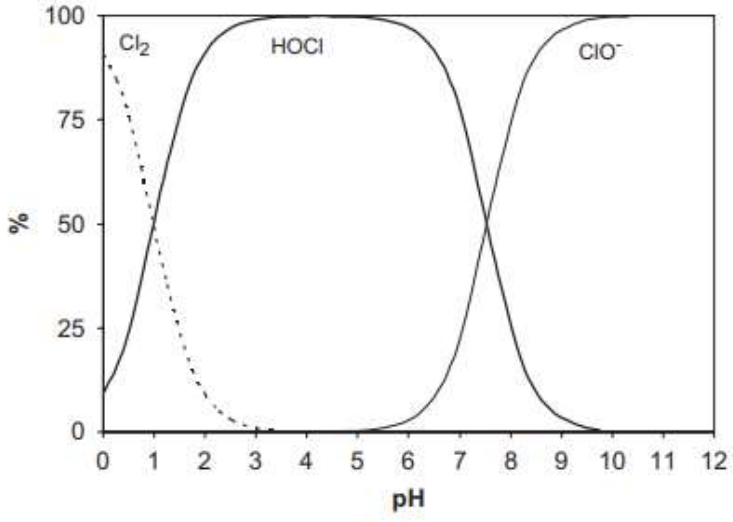

Figure 3.2 - Relative distribution of main aqueous chlorine species as a function of pH at 25 ºC and for a chloride concentration of 5x10^{-3}M (177.5 mg/L) (Reprinted from Deborne and von Gunten [34], Copyright 2008).

Panizza and Cerisola [35] also achieved increasing removal of organics (in terms of COD) for raising current densities from 37 to 62 mA/cm^2 in the treatment of a filtered OMW with a much higher COD (26750 mg O_2 /L versus 718 mg O_2 /L) by AO employing a $TiRuO_2$ anode. After 3 h of reaction, the authors found ~10%, ~18% and ~48% COD removal for 37, 49 and 62 mA/cm^2.

It was decided to use UVC light because it can have two major effects: directly oxidize some organic by-products generated during AO and/or transform some electrogenerated by-products, such as H_2O_2, O_3, $S_2O_8^{2-}$ and HClO, into powerful reactive species, such as $HO^{\bullet}$, $SO_4^{\bullet-}$ and $Cl^{\bullet}$, according to Eqs. (14)-(17). Therefore, there could have been increased degradation of the organic matter present in the effluent if it was susceptible to UVC radiation or attack of the generated oxidants. From the results obtained (Figure 3.1(a)), it seems that in this case this did not happen. The cause of these results can comprise: (i) the non-occurrence of the photolysis of $S_2O_8^{2-}$ and HClO (and H_2O_2 and O_3, although with no confirmation of the presence of these species) because UVC light may have been unable to properly penetrate the effluent in virtue of its dark colour (please see Figure 3.3), (ii) null production of H_2O_2 and O_3 species or their very poor production, being then unable to generate powerful oxidants, (iii) null effect of $Cl^{\bullet}$ produced from HClO on the degradation of the organics of the bio-OMW, and/or (iv) non-susceptibility of organic by-products to the action of UVC light. Figures 3.1(a.1) and 3.1(a.2) show quite similar HClO and $S_2O_8^{2-}$ contents in the absence and presence of UVC light, which corroborates the first hypothesis. According to these results, electrogenerated M($HO^{\bullet}$) and/or HClO/ClO^- may have had a crucial role on organics degradation by AO. The combination of AO with UV irradiation has been studied only to a limited extent but, on opposite to the current results, synergistic effects have been observed when UVC light and AO were used together in the treatment of pure synthetic solutions contaminated with, for example, phenol [36], progesterone [37], and coumarin [38].

In another attempt to enhance the efficiency of AO, Cl^- ions were added to the reaction medium by means of NaCl salt to improve the production of active chlorine species via Eqs. (7)-(9). The content of Cl^- of the effluent was increased from ~0.6 g/L to ~2.4 g/L. In Figure 3.1(a), one can perceive a null improvement on the DOC removal in the presence of a higher Cl^-, which points to a low susceptibility of the organics attending the bio-OMW to the attack of active chlorine species, despite the confirmation of the presence of these species in higher amount – Figure 3.1(a.1) – and the presence of ~50% of HClO – the most powerful active chlorine species (E^o = 1.49 V/SHE) [18] – at the effluent pH (~8). This points to a crucial role of organics oxidation by AO played by electrogenerated M($HO^{\bullet}$). The role of the active chlorine species may not have been large. Figure 3.1(a.2) reveals a larger amount of $S_2O_8^{2-}$ produced during the AO/NaCl compared to the same trial in the absence of salt addition. This value probably corresponds to some interfering agent of the method, likely the additional active chlorine species generated.

The following figure shows the OMW before AO treatment and after various AO treatments (180 min of reaction). The colour changed from dark brown to light yellow after AO treatments at 150 mA/cm^2 and 200 mA/cm^2 (slightly lighter yellow colour at 200 mA/cm^2). The colour of the effluent was visibly almost totally removed in the presence of NaCl, pointing to the conversion of coloured organics into non-coloured compounds.

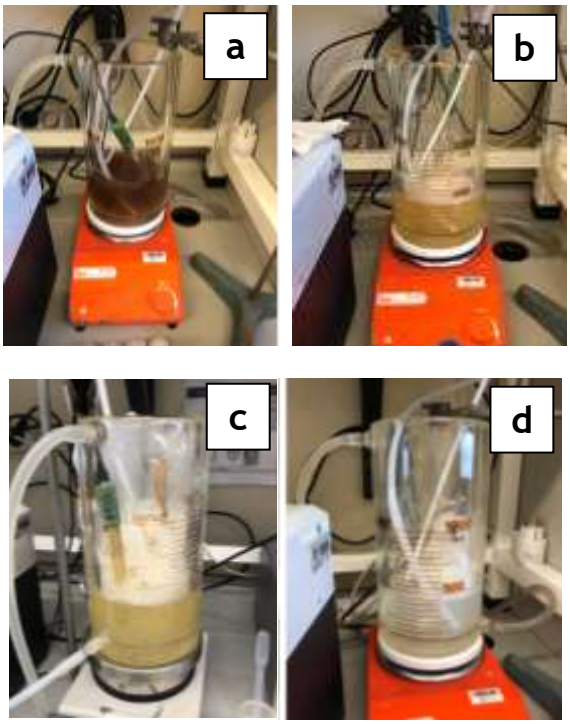

Figure 3.3 - OMW before AO (a), after AO at 150 mA/cm^2 (b), after AO at 200 mA/cm^2 (c), and after AO at 200 mA/cm^2 with added NaCl (d).

Figure 3.4 illustrated the AO processes behaviour as regards energy for electrochemical cell operation. In terms of consumed charge for the electrolysis (Figure 3.4(b)), the DOC decay profiles highly differed from those in terms of electrolysis time. For a same specific charge, the DOC was removed in higher extent for 25 mA/cm^2 and poorly and similarly removed for 100-200 mA/cm^2. One can then infer that, in terms of consumed charge, there was a beneficial effect of a low current density of 25 mA/cm^2 and the absence of adverse effects of applying current densities of 150 and 200 mA/cm^2 compared to 100 mA/cm^2. After a consumed charge of 5.8 Ah/L using 200 mA/cm^2, 30% of DOC removal was achieved. Chatzisymeon et al. [39] achieved 10% COD removal after a consumed charge of ~6 Ah/L using 86 mA/cm^2 in the treatment of a filtered OMW with a much larger content of organics (COD of 40000 mg O_2/L), highly biodegradable, by AO also using a BDD anode.

Figure 3.4(b.1) shows increasing cell voltages for AO processes employing larger current densities, together with similar voltages for AO in the absence and presence of UVC radiation, and a lower voltage for AO with addition of NaCl salt. The EC for the cell to operate (Figure 3.4(b.2)) was directly proportional to the voltage. This means that for lower current densities, the associated energy cost

will be lower too and for higher current densities the opposite, except for the case where NaCl is added to the effluent. The presence of a higher content of ions in the solution bulk, increased the conductivity of the effluent and, consequently, the cell voltage, provides lower energy consumption.

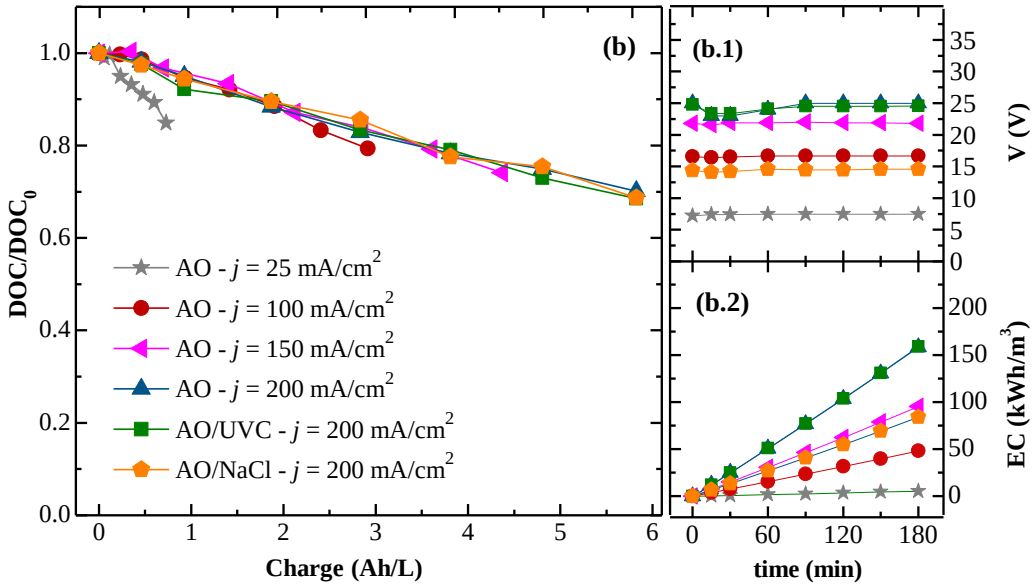

Figure 3.4 - Evolution of normalized DOC removal as a function of consumed specific charge (a), cell voltage as a function of time (a.1) and energy consumption as a function of time (a.2) for the treatment of the bio-OMW by AO. (★) AO at 25 mA/cm^2, (●) AO at 100 mA/cm^2, (◀) AO at 150 mA/cm^2, (▲) AO at 200 mA/cm^2, (■) AO/UVC at 200 mA/cm^2, (⬟) AO/NaCl at 200 mA/cm^2. Operational conditions: pH = natural (7.5-8.4), T = 25 ºC, 11 W UVC lamp, 3.0 g/L NaCl.

It can be concluded that in terms of degradation of organic matter over the 3 h of reaction, one can get a higher degradation for higher current densities, but it must be considered that the energy cost is also higher. Thus, it is important to achieve a balance between these two factors when deciding which is the best current density to use in the experiment.

To verify the characteristics of the effluent after being treated with AO, a characterisation of the OMW obtained at the end of the reaction at 200 mA/cm^2 (180 min) was performed. The results obtained are present in Table 3.2 and Figure 3.5.

According to Table 3.2, the emission limit values (ELV) imposed by Portuguese legislation for the discharge of treated wastewater into the environment (Decree-Law no. 236/98 [40]) were only met for colour and pH. The values obtained for COD, phenols and TSS were above the limits imposed by the legislation. It would be necessary to extend the treatment time by AO or to apply a final biological treatment capable of degrading the organic compounds that changed from recalcitrant to biodegradable with AO. To assess the ability of applying a further biological treatment, a Zhan-Wellens test could be performed using effluent samples at different AO reaction times.

It is worth mentioning that there are other parameters addressed by the law, such as 5-day biological oxygen demand, nitrates, ammonia, among others, that were not analysed.

Table 3.2 - Main characteristics of the OMW after 180 min of AO at 200 mA/cm^2 compared to the bio-OMW.

Parameter	Units	Bio-OMW	After AO	ELV[a]
Colour	-	Dark brown	Light yellow	-
Colour (1:20)	-	d.	n.d.	n.d.
Colour	Pt-Co units	1520	520	-
pH	scale sorënsen	8.1	8.4	6.0-9.0
Conductivity	mS/cm	7.2	6.9	-
Dissolved organic carbon (DOC)	mg C/L	319	223	-
Chemical oxygen demand (COD)	mg O_2/L	718	440	150
COD/DOC	-	2.3	2.0	-
Phenols	mg C_6H_5OH/L	5.3	1.6	0.5
Turbidity	NTU	120	170	-
Total suspended solids (TSS)	mg/L	105	91	60
Volatile suspended solids (VSS)	mg/L	43	35	.

[a] Emission limit values (ELV) for wastewater disposal into aquatic environment imposed by the Portuguese legislation (Decree Law 236/98, 1998).
d. – detected.
n.d. – not detected.

Figure 3.5 - OMW sample before (left) and after (right) AO treatment at 200 mA/cm^2.

3.2 Application of electrochemical processes for production of hydrogen

3.2.1 Membranes characterisation

In this section, standard PBI membrane and PBI membrane with 2 % GO – the membranes used in stability tests for H_2 production (Section 3.2.2) – were characterised. Furthermore, a thermally cured standard PBI membrane, which was not used in the stability tests due to time restrictions, was also characterised. These tests served to characterise better the membranes, to compare the three types of membranes and to understand which is the best one to produce H_2.

- IR and visual aspect

  IR spectroscopy was used to check whether membranes were cured. The spectrum obtained after curing the PBI membrane was compared with the spectrum of a thermally cured membrane present in Aili et al. [33], and with a standard PBI uncured membrane (Figure 3.6). In comparison with the graph of the previously thermally cured membrane, it can be seen that the peaks obtained in the membrane that was cured in this dissertation are very similar. By analysing the spectrum of the two membranes, it can be seen that both showed the same peaks, but these peaks had a higher absorbance for the thermally cured PBI membrane. Thus, it can be concluded that the membrane is cured because there were changes in the IR spectrum of the membrane when compared to a standard uncured membrane.

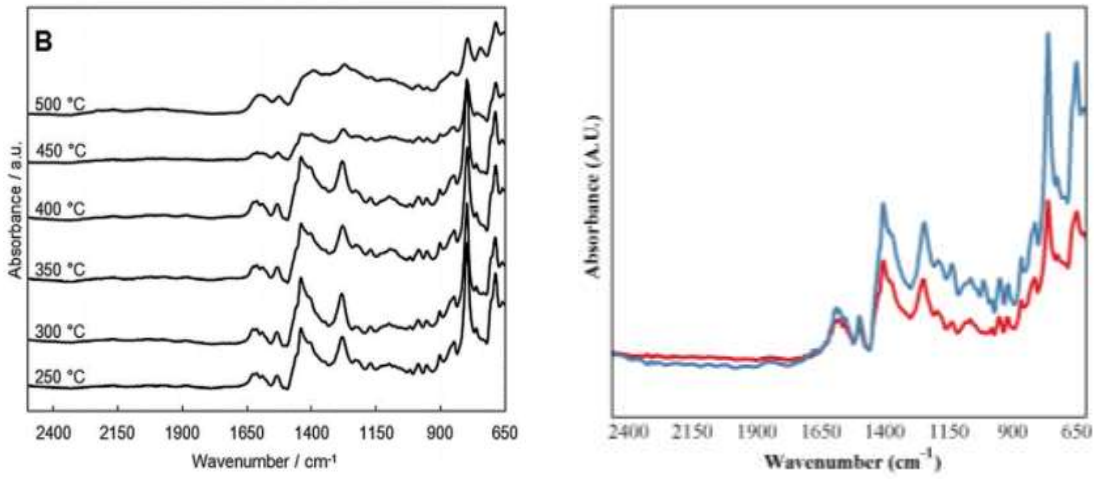

Figure 3.6 - IR spectrum from thermally cured membranes (Reprinted from Aili et al. [33], Copyright 2012) (left) and IR spectrum obtained for (--) thermally cured PBI membrane in this dissertation at 350 ºC and (--) standard PBI membrane (right).

Below, it is presented the visual comparison of the three membranes under study before any test or experiment. As shown in Figure 3.7, the standard membrane when cured became darker. Relative to the membrane that containing GO, this was the darkest membrane since this compound is very dark.

Figure 3.7 - Thermally cured standard PBI membrane, standard PBI membrane, and PBI membrane with 2% GO (from left to right).

- ADL

The ADL for all membranes can be accessed in Table 3.3. The ADL was calculated from Eq. (25) and it is considered that the membrane is well doped when the ADL is above 10. Thus, all membranes were properly doped with H_3PO_4, and highlight can be given to the 2% GO membrane, which presented the highest ADL. It is important to achieve a high ADL, so that the membrane is more conductive, allowing to obtain higher H_2 production. The higher ADL of the 2% GO membrane can be attributed to the GO, which has an OH group, being responsible for facilitating and favouring the entry of H_3PO_4 into the membrane because this acid also contains an OH group. In relation to the thermally cured membrane, it presents the smallest ADL, however it is above 10 and so it can be considered that it is possible to dope the membrane. Table 3.3 also shows that the membrane thickness increased when doped.

Table 3.3 - ADL for the three membranes under study.

Membrane	ADL	Thickness increase (%)
Standard PBI	11.4	106.7
PBI with 2% GO	12.3	119.3
Thermally cured PBI	10.4	162.5

- Retention of H_3PO_4

In the case of H_3PO_4 retention, Table 3.4 shows that the best membrane was again the 2% GO membrane. The standard cured membrane also showed a high percentage of H_3PO_4 retention.

Table 3.4 - Phosphoric acid retention for the three membranes under study.

Membrane	Retention of H_3PO_4 (%)
Standard PBI	25±5
PBI with 2% GO	77±3
Thermally cured PBI	62±11

- Chemical stability to the attack of $S_2O_8^{2-}$

In Table 3.5 are presented the results for the chemical stability of the membranes when subjected to $S_2O_8^{2-}$ attack, to understand which is the most resistant membrane. This test was performed because $S_2O_8^{2-}$ can be formed as by-product of secondary reactions occurring at the anode of the electrochemical cell via Eq. (26) [41].

$$SO_4^{2-} \rightarrow S_2O_8^{2-} + 2e^- \quad (26)$$

Table 3.5 - Membranes (1x1 cm) under study before and after $S_2O_8^{2-}$ attack.

Membrane	Time the membrane held up before breaking	Before and after image
Standard PBI	8 h	
PBI with 2% GO	36 h (1.5 d)	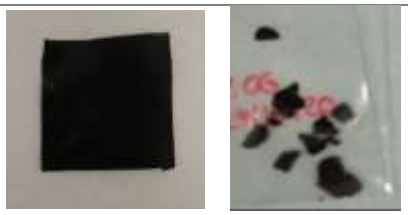
Thermally cured PBI	144 h (6 d)	

The most resistant membrane, with a big difference compared to the others, was the standard PBI cured membrane, followed by the 2% GO membrane and finally the standard PBI membrane. It would be expected that the 2% GO membrane would resist longer than the standard one, because by adding GO the chemical properties of the membrane are improved, as it was seen before. Regarding the

cured membrane, it has been verified that the thermally curing step increases the membrane resistance. Therefore, it can be concluded that thermally curing the membranes also improves some membrane characteristics when compared to standard membrane and even 2% GO membrane.

- Proton conductivity and crossover

In the case of the proton conductivity and crossover, only the results for the standard and 2% GO membranes are presented, as well as for other percentages of GO, in order to present some of the many parameters studied for the choice of the 2% GO percentage. Figures 3.8 and 3.9 were provided by UCLM and were obtained in studies made previously to discover which was the best percentage of GO to be used.

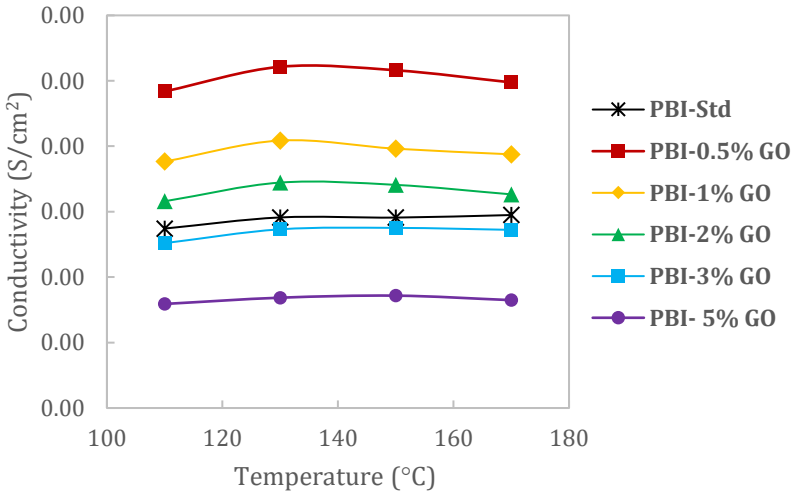

Figure 3.8 - Proton conductivity for standard PBI membrane at various % of GO.

In terms of conductivity, the use of contents of GO from 0.5% to 2% provided better conductivities compared to that of the standard membrane. This can be attributed to the fact that the membranes with GO can achieve higher ADL values, as explained above. The more conductive membrane was that containing 0.5% GO. For higher GO contents, the H_3PO_4 was prevented to enter the membrane, diminishing its conductivity. This occurred because GO is a solid that if it is in too much quantity in the membrane will decrease its porosity and prevent the acid from entering.

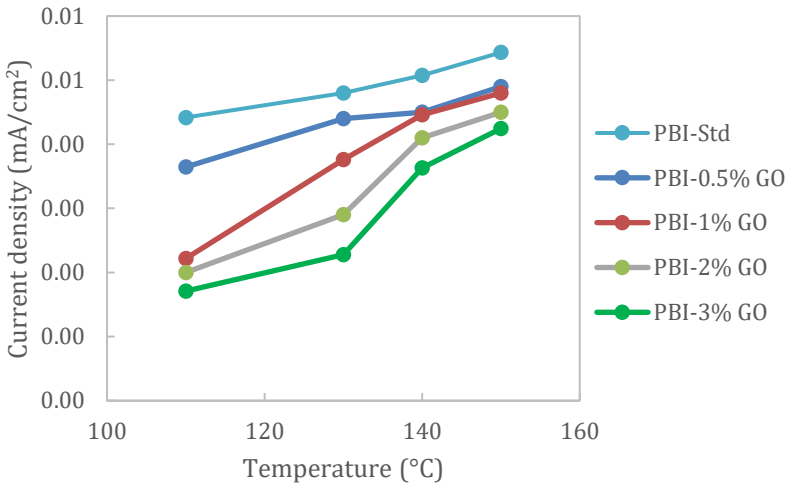

Figure 3.9 - Crossover for standard PBI membrane at various % of GO.

Regarding the crossover, the membrane with the lowest crossover was the 3% GO membrane, which is the best one for this parameter, since less crossover means that there is less SO_2 passing through the membrane. Therefore, combining these two parameters, as well as many others tested and analysed at UCLM, the best percentage of GO was considered to be 2%. Comparing standard and 2% GO, the 2% GO is better again.

3.2.2 Stability tests of membranes with production of hydrogen

Stability tests performed with standard PBI membranes and PBI membranes with 2% GO are presented in this section.

As previously mentioned, before starting the main part of the preliminary stability test, for each membrane two reactions were performed, one at 110 ºC and another at 120 ºC, applying a constant voltage of 0.6 V. These reactions were done just to check if everything was working properly with the cell and the system, if the results obtained were the normal ones and to show how the membrane worked before starting the main experiment.

Firstly, the activation of the system was assessed (Figure 3.10). It was observed that the steady state was reached for 2 A. Then, this was the constant intensity applied in the main part of the stability test.

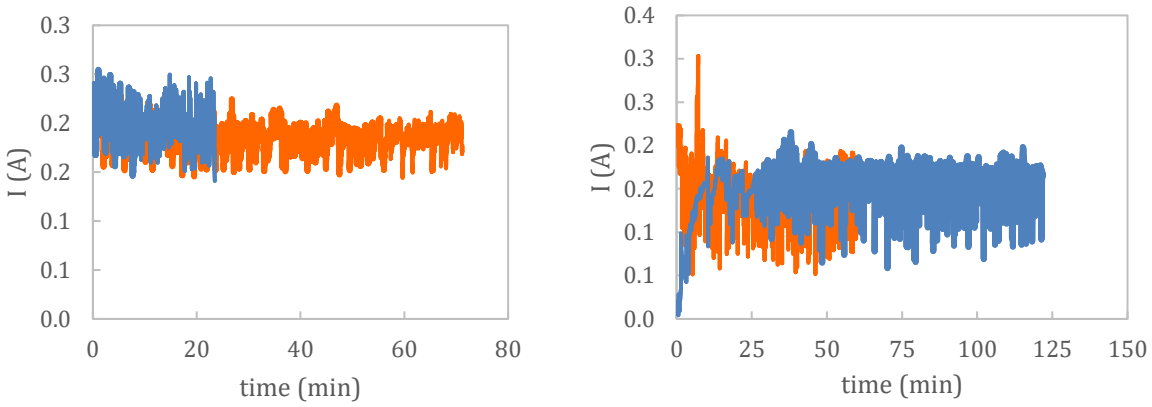

Figure 3.10 - Activation for reaction with standard PBI membrane (left) and PBI membrane with 2% GO (right) for trials at (--) 110 ºC and (--) 120 ºC.

After reaching the steady state, a characterisation of the membranes was made. The flow rates of H_2 and H_2S produced, as well as the efficiency of the reaction calculated via Eq. (27), were assessed (Table 3.6). A high efficiency means that most of the energy supplied to the system is used to produce H_2, and there are few parasitic reactions. Furthermore, polarisation curves (Figure 3.11) and resistances (Table 3.7) were extracted from the software.

$$\text{Efficiency (\%)} = \left(\frac{\text{Flow } H_2 \text{ experimental}}{\text{Flow } H_2 \text{ theoretical}} \right) \times 100 \qquad (27)$$

By analysing Table 3.6 and Figure 3.11, the PBI membrane with 2% GO proved to be better electrochemically than the standard PBI membrane, since it was more efficient, producing higher quantities of H_2 for 120ºC and obtaining higher polarisation curves for both trials. It is important to obtain polarization curves with a high slope because this means that higher current densities can be achieved. If this does not happen and lower current densities are obtained, it means that there may have been a change in the predominant reaction mechanism where parasitic reactions are important, because clearly the performance of the electrolyser is being affected [41].

Table 3.6 - Flow of H_2 and H_2S and respective reaction efficiency for the preliminary reactions at 0.6 V (T = 25 ºC; Pressure = 1 bar).

	Standard PBI			PBI with 2% GO		
T (ºC)	**Flow H_2 (mL/h)**	**Flow H_2S (mL/h)**	**Efficiency (%)**	**Flow H_2 (mL/h)**	**Flow H_2S (mL/h)**	**Efficiency (%)**
110	749.3	1.7	81.0	689.8	2.2	74.5
120	333.7	40.5	36.1	849.0	4.0	91.8

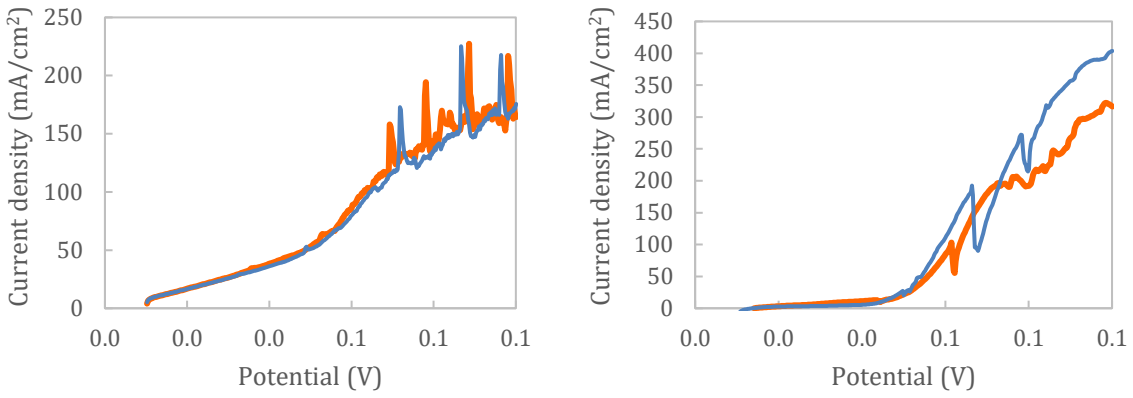

Figure 3.11 - Polarisation curves for reaction with standard PBI membrane (left) and PBI membrane with 2% GO (right) for trials at (--) 110 ºC and (--) 120 ºC.

Since the H_2S production was similar in both membranes at 110 ˚C, but much higher in the standard PBI membrane at 120 ˚C, this proves once again that the 2% GO membrane is better because less secondary reactions occur, where H_2S is produced. GO improves properties such as acid doping and proton conductivity, among other properties, all of which are presented below throughout the results and discussion [42].

Regarding the different temperatures, it is expected that for 110 ºC the process is more efficient, since with the increase of temperature, the H_2 production decreases and the H_2S production increases, which was verified for the standard membrane. In the case of the 2% GO membrane at 120ºC, there was a higher production of H_2. This may have happened because at 110 ºC the steady state was not fully reached, and it would take a little longer.

Normally, these processes work at a lower temperature, such as 80 ºC. One of the novel things of this study is to be able to work at those high temperatures.

Resistance values (Table 3.7) were obtained for a constant voltage applied to the system of 0.7 V. R_s or R_Ω, ohmic resistance, corresponds to the series resistance made by the materials: electrode, membrane, and connections. The membrane is the most important and the most significant. R_s is considered the real resistance of the system. The charge transfer resistance, R_p or R_{ch}, corresponds to a more abstract resistance, which gives an idea about the reactions and it is the resistance required for the reaction to occur.

For the 2% GO membrane, the R_p values obtained were much lower than those for the standard membrane. That can be attributed to the higher proton conductivity of the PBI with 2% GO membrane when compared with a standard membrane. The proton transport was enhanced and so the reactions.

As has been said, the charge transfer resistance is the resistance for the reactions to occur. So, with a better proton conductivity, the kinetics are enhanced and the resistance for the reactions is lower.

Table 3.7 - Resistances obtained when a voltage of 0.7 V was applied to the system.

	Standard PBI		PBI with 2% GO	
T (°C)	**R_s (mΩ)**	**R_p (mΩ)**	**R_s (mΩ)**	**R_p (mΩ)**
110	8.51	121	18.4	27.5
120	8.46	160	18.3	39.3

Next, the main part of the stability test was started, where a constant current intensity of 2 A was applied (current density of 80 mA/cm^2) together with a constant temperature of 120 ºC. The results are presented below.

Figure 3.12 and 3.13 show the potential profile over the days of the stability tests for each membrane. For the standard membrane (Figure 3.12), the end of each day was marked, where the reaction was stopped and restarted the next day morning, and the characterisations made over time. For this membrane, it was verified that the voltage never exceeded 1 V, that is, the membrane never broke throughout the stability test.

At the beginning of a new day, the voltage obtained was always lower than the day before, because during the night, as the experiment was stopped, the membrane recovered a little.

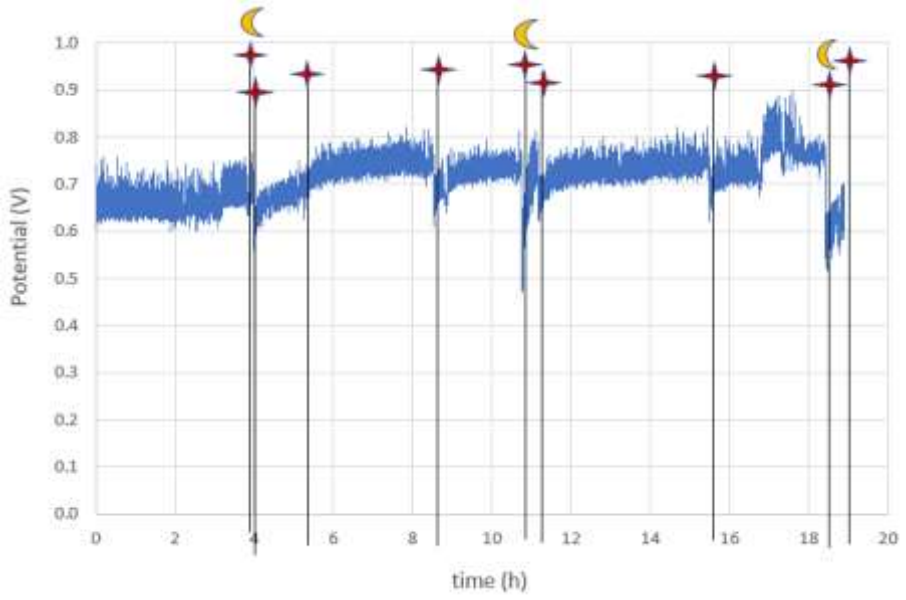

Figure 3.12 - Potential profile over the days of the stability test for standard PBI membrane when applying a constant current density of 80 mA/cm^2. (☾) end of a day and (✦) characterisation.

In the case of the 2% GO membrane, it broke on the first day, 37 min after the start of the stability test, as shown in Figure 3.13, as at around 37 min the voltage increased abruptly, passing 1 V. This happened because, although the membrane with GO was much better electrochemically (obtaining greater amounts of H_2 and better results) as evidenced in trials for 110 ºC and 120 ºC, mechanically it was weaker. The fact that the membranes under study had a very thin thickness (40 µm) and the fact of adding GO (2%) to the composition of the membrane, which is a solid, leads to the membrane to be more fragile and more rigid, losing mechanical stability for this thickness, when compared with the standard membrane. Figure 3.14 shows the visual aspect of the PBI membrane with 2% GO after the test.

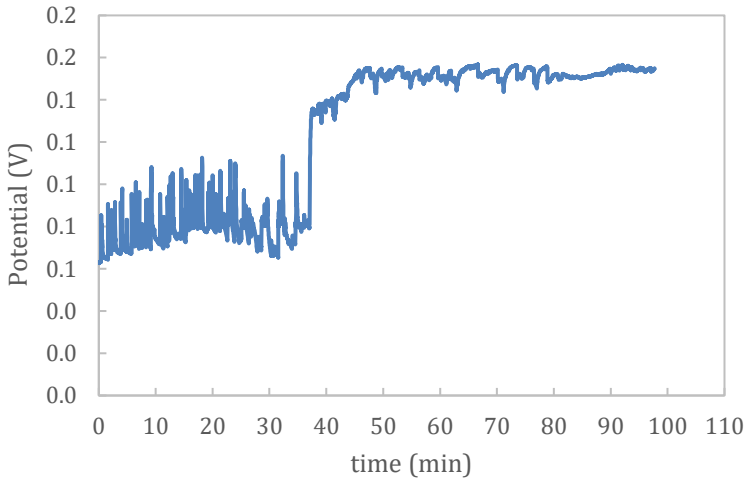

Figure 3.13 - Potential profile over the days of the stability test for PBI membrane with 2% GO when applying a constant current density of 80 mA/cm^2.

Figure 3.14 - Burnt electrode at the end of the stability test for the PBI membrane with 2% GO.

Table 3.8 show the flow of H_2 and H_2S produced and the respective efficiency for each characterisation performed during the stability test for the standard PBI membrane. Since the 2% GO membrane ruptured quite early, there is only one reading of the produced amount of H_2 and H_2S (Table 3.9).

Table 3.8 - Flow of H_2 and H_2S and respective efficiency for each characterisation performed during the stability test for the standard PBI membrane (T = 25 ºC; Pressure = 1 bar).

Time (h)	Flow of H_2 (mL/h)	Flow of H_2S (mL/h)	Ratio H_2/H_2S	Efficiency (%)
3.97	411.2	1.6	257.0	44.4
3.97	424.8	37.1	11.4	45.9
5.25	407.5	37.6	10.8	44.0
8.52	277.2	14.2	19.5	30.0
10.76	296.2	11.7	25.3	32.0
11.18	250.0	20.3	12.3	27.0
15.50	259.3	22.4	11.6	28.0
18.43	82.8	24.8	3.3	9.0
18.91	81.3	25.2	3.2	8.8

Table 3.9 - Flow of H_2 and H_2S and respective efficiency during the stability test for the PBI membrane with 2% GO (T = 25 ºC; Pressure =1 bar).

Flow of H_2 (mL/h)	Flow of H_2S (mL/h)	Efficiency (%)
732.9	19.1	79.2

By analysing the Table 3.8, it can be seen that over time more H_2S and less H_2 started to be produced, which is why the stability test was terminated (the value considered for the production of H_2 to be profitable was a flow greater than 100 mL/h). The reason for this change in production of the compound, is the accumulation of sulfur on the cathode side. During the whole reaction there is always crossover, that is, there is always some SO_2 that passes through the membrane, from the anode to the cathode. Theoretically, the crossover is constant over the reaction time, because it only varies with the variation of temperature (more temperature, more crossover, because with the increase of temperature, the membrane is damaged faster and more SO_2 passes the membrane), and with the thickness of the membrane (more thickness, less crossover, because in a thicker membrane it is harder to SO_2 to pass through). Thus, it is concluded that, the crossover does not increase over time, unless the membrane breaks or there are large holes (which did not happen in the stability test, because the resistances of the electrolysis system is stable). So, it can be considered that the crossover was constant throughout the experiment, but over time the amount of sulphur that accumulated on the cathode side increased and for this reason, at the end of 19 h of reaction, a large amount of sulfur has accumulated on the cathode side which starts to favour the following reactions on the cathode (Eq. (28)-(29)):

$$SO_2\,(g) \rightarrow S\,(g) + O_2\,(g) \quad (28)$$

$$S\,(g) + H_2\,(g) \rightarrow H_2S\,(g) \quad (29)$$

In addition, the following reaction also occurs at the cathode, which is responsible for the formation of H_2, Eq. (30), but over time the hydrogen molecule begins to react with the sulphur accumulated at

the cathode via Eq. (29), and the reaction where H_2S is formed begins to occur in higher extent, thus increasing its production.

$$2\ H^+ \rightarrow H_2\ (g) \qquad (30)$$

The efficiency decreased throughout the stability test because less H_2 and more H_2S were produced. So, the voltage that was supplied to the system was no longer used to produce H_2 and started to be used to produce H_2S over time.

Comparing the H_2 production in the two membranes, it can again be seen that electrochemically the 2% GO membrane was much better, obtaining much higher H_2 productions (Table 3.9).

Regarding the resistances presented below (Figure 3.15), they only indicate that the electrolysis system for the standard membrane was stable throughout the stability test and even at the end of the 19 h of operation. This is because the values obtained for the resistances, R_s and R_p, did not suffer great variations and may be considered constant over the time. Being stable means that electrochemically the system was working well, without membrane rupture and without degradation of the electrodes, as previously mentioned.

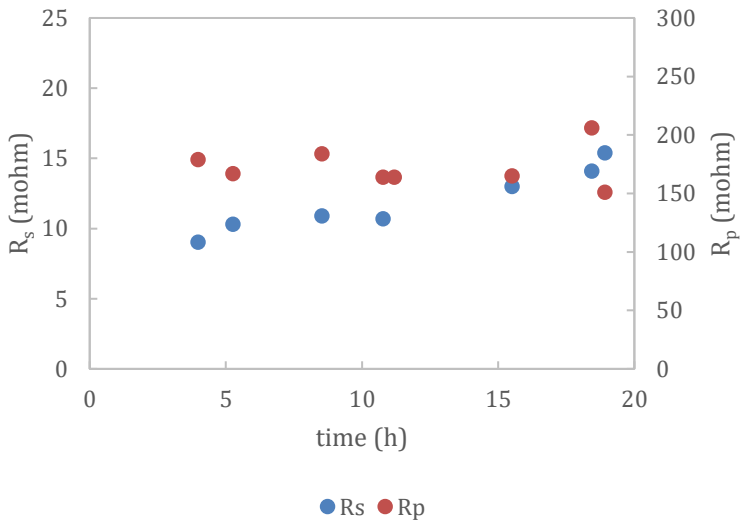

Figure 3.15 - Resistances obtained in the characterisations made during the stability test for standard PBI membrane when a voltage of 0.7 V was applied to the system.

For the 2% GO membrane, as it broke shortly after the stability test started, no resistance values were obtained during the main part of the stability test. But one would expect the R_Ω to be similar to those of the standard membrane and the R_{ch} to be lower, as explained above.

Regarding the polarisation curves (Figure 3.16), they were very similar during the stability test for the standard PBI membrane, which also indicates that the electrolysis system is electrochemically stable.

For the 2% GO membrane, no polarization curves could be obtained due to the membrane rupture. But it would be expected that the polarization curves would reach higher values of current density for the same applied voltage (0-1 V), indicating a better efficiency since this membrane is better electrochemically than the standard, as already seen in the trials performed before the main stability test.

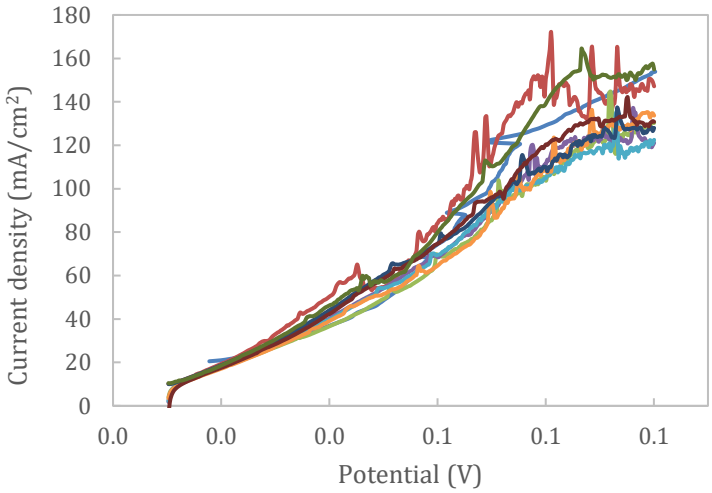

Figure 3.16 - Polarisation curves for each characterisation made during the stability test for standard PBI membrane. (--) t=3.97 h, (--) t=3.97 h, (--) t=5.25 h, (--) t=8.52 h, (--) t=10.77 h, (--) t=11.18 h, (--) t=15.50 h, (--) t=18.43 h, (--) t=18.91 h.

In the Appendix A, it can be found analyses performed on the cathode and anode purge for each of the stability tests with the two types of membranes. In these analyses, phosphates (PO_4^{3-}) and sulphates (SO_4^{2-}) were measured. The electrodes and the membrane were doped with H_3PO_4, and so it is expected that there are some PO_4^{3-} in the residues at the anode and cathode that were released in the electrochemical cell. SO_4^{2-} are produced from reactions with SO_2. It can be concluded that in the stability test for both the standard membrane and the 2% GO membrane, SO_4^{2-} were present at the anode and cathode. However, PO_4^{3-} were absent from the anode of the standard membrane.

4 Conclusions

4.1 Application of electrochemical processes for wastewater treatment

AO proved to be a suitable process for the remediation of the pre-treated OMW. After 3 h of reaction, organics removals, in terms of DOC decay, of 15%, 21%, 26% and 30% were obtained for current densities of 25, 100, 150 and 200 mA/cm^2. This higher degradation for larger current densities was accompanied by a higher energy consumption for electrochemical cell operation, pointing to the need for stablishing a balance between these two factors when selecting the best current density. The use of UVC light and the addition of a salt (NaCl) to the wastewater did not improve the efficiency of the AO process. The $HO^{\bullet}$ electrogenerated at the anode (BDD) surface proved to play a crucial role on organics oxidation by AO. Upon 3 h of AO at 200 mA/cm^2, the legal requirements for the direct discharge of treated OMW into water bodies could not be achieved for all parameters evaluated, which is a major challenge regarding OMW remediation. The legal requirements were only met for colour and pH. So, it would be necessary to extend the treatment time by AO or to apply a final biological treatment process capable of degrading the organic compounds that changed from recalcitrant to biodegradable with AO.

4.2 Application of electrochemical processes for production of hydrogen

The PBI membrane with 2% GO promoted the production of higher amounts of H_2 and lower amounts of undesired H_2S by PEM electrolysis compared to a standard PBI membrane, ultimately leading to a higher process efficiency. However, the new membrane was not stable for the thickness used, since it only held 37 min in the stability test before rupturing, contrasting with a very good stability achieved for the standard PBI membrane. The GO in the membrane conferred rigidity to the membrane and then the new membrane had lost mechanically stability for this thickness compared to the standard PBI membrane.

The higher efficiency for H_2 production achieved for the PBI membrane with 2% GO can be attributed to its higher content of H_3PO_4 (dopant) and higher capacity to retain this compound, thereby contributing to a higher conductivity. According to the chemical stability test to the attack of $S_2O_8^{2-}$, a reaction by-product, the PBI membrane with 2% GO would be more stable than the standard PBI membrane, which contrasts with the mechanical stability.

The characterization of a third membrane, a thermally cured PBI membrane, revealed its higher capability, mainly as regards chemical stability.

5 Assessment of the work done

5.1 Objectives achieved

The main objectives achieved with this work were:

1. Successful application of an electrochemical process, AO, to the remediation of OMW, allowing a good degradation of organics, even though it would be necessary to extend the AO process or couple a subsequent biological treatment to meet the discharge limits;
2. Successful application of PEM electrolysis for the generation of H_2 using an innovative PBI membrane with 2% GO, since it has demonstrated stability when subjected to high temperatures and current densities for a long period of time, along with high H_2 generation;
3. Discovery of very promising characteristics of thermally cured PBI membranes.

5.2 Other work carried out

At the beginning of the work at the UCLM, studies with sulphonated membranes were attempted, since sulphonating the membranes improves some of their properties. This was not possible because these membranes could not be doped as they have broken when placed in phosphoric acid.

5.3 Final assessment and suggestions for future work

The work done provided very interesting information regarding environmental remediation since the disposal of the effluent under study is a major problem. Another approach made in this work was the production of H_2 through the Westinghouse cycle, using PEM, which showed to be a very efficient and promising process since the use of green H_2 as the main energy to replace fossil fuels has been increasing exponentially worldwide.

Thermally cured PBI membranes showed very promising characteristics in the tests performed and there was no time to perform stability tests for these membranes. Thus, the suggestion for future work is to conduct stability studies for the thermally cured PBI membranes.

6 References

[1] R. Elkacmi and M. Bennajah, "Advanced oxidation technologies for the treatment and detoxification of olive mill wastewater: A general review" *J. Water Reuse Desalin.*, vol. 9, no. 4, pp. 463–505, 2019, doi: 10.2166/wrd.2019.033.

[2] International Renewable Energy Agency (IRENA), "Renewable energy in the water, energy and food nexus" pp. 1–125, 2015.

[3] M. P. Alberto Gandolfi, Ajay Patel, Michele Della Vigna, and Mafalda Pombeiro, "Green Hydrogen: The next transformational driver of the hydrogen utilities industry" Goldman Sachs Group, Inc., Equity Research, 2020.

[4] Y. Liu, Y. Y. Deng, Q. Zhang, and H. Liu, "Overview of recent developments of resource recovery from wastewater via electrochemistry-based technologies" *Sci. Total Environ.*, vol. 757, p. 143901, 2021, doi: 10.1016/j.scitotenv.2020.143901.

[5] F. C. Moreira, R. A. R. Boaventura, E. Brillas, and V. J. P. Vilar, "Electrochemical advanced oxidation processes: A review on their application to synthetic and real wastewaters" *Appl. Catal. B Environ.*, vol. 202, pp. 217–261, 2017, doi: 10.1016/j.apcatb.2016.08.037.

[6] M. M. Rashid, M. K. Al Mesfer, H. Naseem, and M. Danish, "Hydrogen production by water electrolysis: a review of alkaline water electrolysis, PEM water electrolysis and high temperature water electrolysis" *Int. J. Eng. Adv. Technol.*, no. 3, pp. 2249–8958, 2015.

[7] P. V. Nidheesh, D. Syam Babu, B. Dasgupta, P. Behara, B. Ramasamy, and M. Suresh Kumar, "Treatment of arsenite- contaminated water by electrochemical advanced oxidation processes" *ChemElectroChem*, vol. 7, no. 11, pp. 2418–2423, 2020, doi: 10.1002/celc.202000549.

[8] R. Dewil, D. Mantzavinos, I. Poulios, and M. A. Rodrigo, "New perspectives for advanced oxidation processes" *J. Environ. Manage.*, vol. 195, pp. 93–99, 2017, doi: 10.1016/j.jenvman.2017.04.010.

[9] M. A. R. C. Barrera-Díaz, P. Cañizares, F.J. Fernández, R. Natividad, "Electrochemical advanced oxidation processes: an overview of the current applications to actual industrial effluents" *AIChE Annu. Meet. Conf. Proc.*, vol. 58, no. 3, pp. 256–275, 2008.

[10] F. Kaplan, A. Hesenov, B. Gözmen, and O. Erbatur, "Degradations of model compounds representing some phenolics in olive mill wastewater via electro-Fenton and photoelectro-Fenton treatments" *Environ. Technol.*, vol. 32, no. 7, pp. 685–692, 2011, doi: 10.1080/09593330.2010.510536.

[11] F. A. El-Gohary, M. I. Badawy, M. A. El-Khateeb, and A. S. El-Kalliny, “Integrated treatment of olive mill wastewater (OMW) by the combination of Fenton’s reaction and anaerobic treatment” *J. Hazard. Mater.*, vol. 162, no. 2–3, pp. 1536–1541, 2009, doi: 10.1016/j.jhazmat.2008.06.098.

[12] N. Flores, P. L. Cabot, F. Centellas, J. A. Garrido, R. M. Rodríguez, and I. Sirés, “4-Hydroxyphenylacetic acid oxidation in sulfate and real olive oil mill wastewater by electrochemical advanced processes with a boron-doped diamond anode” *Cell*, vol. 24545, pp. 1–5, 2001, doi: 10.1016/j.jhazmat.2016.09.057

[13] L. C. Davies, A. M. Vilhena, J. M. Novais, and S. Martins-Dias, “Olive mill wastewater characteristics: Modelling and statistical analysis” *Grasas y Aceites*, vol. 55, no. 3, pp. 233–241, 2004, doi: 10.3989/gya.2004.v55.i3.171.

[14] K. Pelendridou, M. K. Michailides, D. P. Zagklis, A. G. Tekerlekopoulou, C. A. Paraskeva, and D. V. Vayenas, “Treatment of olive mill wastewater using a coagulation-flocculation process either as a single step or as post-treatment after aerobic biological treatment” *J. Chem. Technol. Biotechnol.*, vol. 89, no. 12, pp. 1866–1874, 2014, doi: 10.1002/jctb.4269.

[15] Y. Bar Oz *et al.*, “Treatment of olive mill wastewater using ozonation followed by an encapsulated acclimated biomass” *J. Environ. Chem. Eng.*, vol. 6, no. 4, pp. 5014–5023, 2018, doi: 10.1016/j.jece.2018.07.003.

[16] G. Hodaifa, J. M. Ochando-Pulido, S. Rodriguez-Vives, and A. Martinez-Ferez, “Optimization of continuous reactor at pilot scale for olive-oil mill wastewater treatment by Fenton-like process” *Chem. Eng. J.*, vol. 220, pp. 117–124, 2013, doi: 10.1016/j.cej.2013.01.065.

[17] M. Panizza and G. Cerisola, “Direct and mediated anodic oxidation of organic pollutants” *Chem. Rev.*, no. 12, pp. 6541–6569, 2009, doi: 10.1021/cr9001319.

[18] D. C. Harris, "Exploring Chemical Analysis", 4th ed., W. H. Freeman and Company, New York, United States, 2009.

[19] P. A. Michaud, M. Panizza, L. Ouattara, T. Diaco, G. Foti, and C. Comninellis, “Electrochemical oxidation of water on synthetic boron-doped diamond thin film anodes” *J. Appl. Electrochem.*, vol. 33, no. 2, pp. 151–154, 2003, doi: 10.1023/A:1024084924058.

[20] L. W. Matzek and K. E. Carter, “Activated persulfate for organic chemical degradation: A review” *Chemosphere*, vol. 151, pp. 178–188, 2016, doi: 10.1016/j.chemosphere.2016.02.055.

[21] P. Devi, U. Das, and A. K. Dalai, “In-situ chemical oxidation: Principle and applications of peroxide and persulfate treatments in wastewater systems” *Sci. Total Environ.*, vol. 571, pp. 643–657, 2016, doi: 10.1016/j.scitotenv.2016.07.032.

[22] J. H. Baxendale and J. A. Wilson, “The photolysis of hydrogen peroxide at high light intensities” *Trans. Faraday Soc.*, vol. 53, pp. 344–356, 1957, doi: 10.1039/tf9575300344.

[23] M. A. Tarr, "Chemical Degradation Methods for Wastes and Pollutants", CRC Press, New Orleans, Louisiana, U.S.A,+ 2003.

[24] L. Dogliotti and E. Hayon, “Flash Photolysis of Persulfate Ions in Aqueous Solutions”, Pioneering Research Division, U. S. Army Natick Laboratories, Natick, Massachusetts, 1966.

[25] Y. Feng, D. W. Smith, and J. R. Bolton, “Photolysis of aqueous free chlorine species (HOCl and OCl^-) with 254 nm ultraviolet light” *J. Environ. Eng. Sci.*, vol. 6, no. 3, pp. 277–284, 2007, doi: 10.1139/S06-052.

[26] M. Gotsi, N. Kalogerakis, E. Psillakis, P. Samaras, and D. Mantzavinos, “Electrochemical oxidation of olive oil mill wastewaters” *Water Res.*, vol. 39, no. 17, pp. 4177–4187, 2005, doi: 10.1016/j.watres.2005.07.037.

[27] S. Díaz-Abad, M. Millán, M. A. Rodrigo, and J. Lobato, “Review of anodic catalysts for SO_2 depolarized electrolysis for ‘green hydrogen’ production” *Catalysts*, vol. 9, no. 1, 2019, doi: 10.3390/catal9010063.

[28] M. Carmo, D. L. Fritz, J. Mergel, and D. Stolten, “A comprehensive review on PEM water electrolysis” *Int. J. Hydrogen Energy*, vol. 38, no. 12, pp. 4901–4934, 2013, doi: 10.1016/j.ijhydene.2013.01.151.

[29] M. Mamlouk and K. Scott, “The effect of electrode parameters on performance of a phosphoric acid-doped PBI membrane fuel cell” *Int. J. Hydrogen Energy*, vol. 35, no. 2, pp. 784–793, 2010, doi: 10.1016/j.ijhydene.2009.11.027.

[30] F. C. Moreira *et al.*, “Selecting the best piping arrangement for scaling-up an annular channel reactor: An experimental and computational fluid dynamics study” *Sci. Total Environ.*, vol. 667, pp. 821–832, 2019, doi: 10.1016/j.scitotenv.2019.02.260.

[31] American Public Health Association, American Water Works Association, and Water Environment Federation, “Part 3000 Metals. 3111 Metals by Flame Atomic Absorption Spectrometry. 3111 B Direct Air - Acetylene Flame Method” *Stand. Methods Exam. Water Waste Water*, pp. 3–104, 1992, [Online]. Available: https://www.standardmethods.org/.

[32] C. Liang, C. F. Huang, N. Mohanty, and R. M. Kurakalva, “A rapid spectrophotometric determination of persulfate anion in ISCO” *Chemosphere*, vol. 73, no. 9, pp. 1540–1543, 2008, doi: 10.1016/j.chemosphere.2008.08.043.

[33] D. Aili, L. N. Cleemann, Q. Li, J. O. Jensen, E. Christensen, and N. J. Bjerrum, “Thermal curing of PBI membranes for high temperature PEM fuel cells” *J. Mater. Chem.*, vol. 22, no. 12, pp.

5444–5453, 2012, doi: 10.1039/c2jm14774b.

[34] M. Deborde and U. von Gunten, "Reactions of chlorine with inorganic and organic compounds during water treatment-Kinetics and mechanisms: A critical review" *Water Res.*, vol. 42, no. 1–2, pp. 13–51, 2008, doi: 10.1016/j.watres.2007.07.025.

[35] M. Panizza and G. Cerisola, "Olive mill wastewater treatment by anodic oxidation with parallel plate electrodes" *Water Res.*, vol. 40, no. 6, pp. 1179–1184, 2006, doi: 10.1016/j.watres.2006.01.020.

[36] G. Hurwitz, P. Pornwongthong, S. Mahendra, and E. M. V. Hoek, "Degradation of phenol by synergistic chlorine-enhanced photo-assisted electrochemical oxidation" *Chem. Eng. J.*, vol. 240, pp. 235–243, 2014, doi: 10.1016/j.cej.2013.11.087.

[37] M. J. M. De Vidales, S. Barba, C. Sáez, P. Cañizares, and M. A. Rodrigo, "Coupling ultraviolet light and ultrasound irradiation with conductive-diamond electrochemical oxidation for the removal of progesterone" *Electrochim. Acta*, vol. 140, pp. 20–26, 2014, doi: 10.1016/j.electacta.2014.02.118.

[38] D. Montanaro, R. Lavecchia, E. Petrucci, and A. Zuorro, "UV-assisted electrochemical degradation of coumarin on boron-doped diamond electrodes" *Chem. Eng. J.*, vol. 323, pp. 512–519, 2017, doi: 10.1016/j.cej.2017.04.129.

[39] E. Chatzisymeon, N. P. Xekoukoulotakis, E. Diamadopoulos, A. Katsaounis, and D. Mantzavinos, "Boron-doped diamond anodic treatment of olive mill wastewaters: Statistical analysis, kinetic modeling and biodegradability" *Water Res.*, vol. 43, no. 16, pp. 3999–4009, 2009, doi: 10.1016/j.watres.2009.04.007.

[40] Ministério do Ambiente, "Decreto-Lei n.º 236/98" *Diário da República n.º 176/1998, Série I-A 1998-08-01*, vol. Nº 176, pp. 3676–3722, 1998, [Online]. Available: https://dre.pt/application/conteudo/430457.

[41] S. Díaz-Abad, M. A. Rodrigo, and J. Lobato, "First approaches for hydrogen production by the depolarized electrolysis of SO_2 using phosphoric acid doped polybenzimidazole membranes" *Int. J. Hydrogen Energy*, vol. 46, no. 58, pp. 29763–29773, 2021, doi: 10.1016/j.ijhydene.2021.06.117.

[42] N. Üregen, K. Pehlivanoğlu, Y. Özdemir, and Y. Devrim, "Development of polybenzimidazole/graphene oxide composite membranes for high temperature PEM fuel cells" *Int. J. Hydrogen Energy*, vol. 42, no. 4, pp. 2636–2647, 2017, doi: 10.1016/j.ijhydene.2016.07.009.

Appendix A - Analyses performed on the cathode and anode purge

For each stability test with different membranes, over time samples were taken from the anode and cathode purges to measure the amount of sulphate (SO_4^{2-}) and phosphates (PO_4^{3-}). The results obtained are presented in Tables A.6.1 and A.6.2.

Table A.6.1 - Samples and purges taken from the anode and cathode purges for stability test with standard PBI membrane.

	T (°C)	V (mL)		PO_4^{3-} (mg/L)		SO_4^{2-} (mg/L)	
		Anode	Cathode	Anode	Cathode	Anode	Cathode
Preliminary test - 0.6 V	110	6.1	6.6	0	1791	55730	8852
	120	5.0	4.2	0	127	48404	1296
Stability test – 2 A	120	6.2	7.2	0	172	54029	12270
	120	4.4	6.0	0	750	57580	128210
	120	6.6	7.4	0	0	54527	1555
	120	5.4	4.8	0	0	52151	382
	120	7.0	15.0	0	199	23086	4197
	120	5.2	5.2	0	0	30270	652
	120	1.6	0.6	0	0	46350	34300
	120	2.3	0.9	0	0	82582	6747

Table A.6.2 - Samples taken from the anode and cathode purges for stability test with PBI membrane with 2% GO.

	T (°C)	V (mL)		PO_4^{3-} (mg/L)		SO_4^{2-} (mg/L)	
		Anode	Cathode	Anode	Cathode	Anode	Cathode
Preliminary test - 0.6 V	110	2.6	5.3	880	235	41499	103040
	120	3.6	10.0	0	141	22831	68604
Stability test – 2 A	120	3.0	5.4	805	172	23055	18168

Figure A.6.1 - Samples for stability test for PBI membrane with 2% GO from cathode (C) and anode (A) purge.